**≋USGS**
*science for a changing world*

Ecosystems Mission Area—Species Management Research Program

Prepared in cooperation with the U.S. Navy

# Black Abalone Surveys at Naval Base Ventura County, San Nicolas Island, California: 2021, Annual Report



Open-File Report 2022–1107

**U.S. Department of the Interior**
**U.S. Geological Survey**

# Black Abalone Surveys at Naval Base Ventura County, San Nicolas Island, California: 2021, Annual Report

By Michael C. Kenner and Julie L. Yee

Open-File Report 2022–1107

**U.S. Department of the Interior**
**U.S. Geological Survey**

U.S. Geological Survey, Reston, Virginia: 2022

# Acknowledgments

# Contents

# Figures

## Tables

## Conversion Factors

International System of Units to U.S. customary units

| Multiply | By | To obtain |
|---|---|---|
| Length | | |
| centimeter (cm) | 0.3937 | inch (in.) |
| millimeter (mm) | 0.03937 | inch (in.) |
| meter (m) | 3.281 | foot (ft) |
| meter (m) | 1.094 | yard (yd) |
| Area | | |
| square meter (m$^2$) | 0.0002471 | Acre |
| Weight | | |
| kilogram (kg) | 2.20462 | Pounds (lbs) |

# Abbreviations

| | |
|---|---|
| CaXc | *Candidatus* Xenohaliotis californiensis; a Rickettsiales-like prokaryotic organism identified as the causative agent in withering syndrome |
| GAM | generalized additive model |
| SNI | San Nicolas Island |
| WS | withering syndrome |

# Black Abalone Surveys at Naval Base Ventura County, San Nicolas Island, California: 2021, Annual Report

By Michael C. Kenner and Julie L. Yee

## Abstract

The U.S. Geological Survey monitors a suite of intertidal black abalone sites at San Nicolas Island, California, in cooperation with the U.S. Navy, which owns the island. The nine rocky intertidal sites were established in 1980 to study the potential effect of translocated sea otters on the intertidal black abalone population at the island. The sites were monitored from 1981 to 1997, usually annually or biennially. Monitoring resumed in 2001 and has been completed annually since then. Since 2018, the work has been carried out by the U.S. Geological Survey Western Ecological Research Center. The study sites became particularly important, from a management perspective, after a virulent disease decimated black abalone populations throughout southern California beginning in the mid-1980s. The disease, withering syndrome, was first observed on San Nicolas Island in 1992 and during the next few years, it reduced the population there by more than 99 percent. The species was subsequently listed as endangered under the Endangered Species Act in 2009.

The subject of this report is the 2021 survey of the sites and how the measured population status compares to the long-term data (collected over several decades) at San Nicolas Island. During the last two decades, the total monitored black abalone population at the island has grown approximately ten-fold after the disease related decline, from about 200 to more than 2,000 abalone. Since it was first consistently measured in 2005, the mean distance between adjacent black abalone has decreased substantially from approximately 50 centimeters to less than 15 centimeters, indicating that abalone are close enough together at several of the sites to reproduce successfully. The 2021 counts were the first since 2016 to indicate a possible decline in the monitored population at San Nicolas Island. Although still more than ten times the population counted in 2001, counts on the transects dropped by 13.6 percent from the survey count in 2020. The most significant decline was the loss of 341 abalone, from the previous count of 547, on a transect that since 2002 had the highest count of all 44 transects. Between 2020 and 2021, there were increases and decreases at the sites and the transects at each site. Although the 2021 count was lower than the 2020 count, it was the second highest since 1997. Based on the number of small abalone counted, recruitment rates were similar to most years since 2008 and higher than the rates observed before the population declines resulting from withering syndrome.

## Introduction

### Haliotis

The black abalone (*Haliotis cracherodii*) is one of seven species of *Haliotis* endemic to the west coast of North America and present in California waters (California Department of Fish and Game, 2004). The other *Haliotis* species that are native to California are the green abalone (*H. fulgens*), the red abalone (*H. rufescens*), the pink abalone (*H. corrugata*), the white abalone (*H. sorenseni*), the pinto abalone (*H. kamtschatkana*) and the flat abalone (*H. walallensis*). There are 55 species and several subspecies of *Haliotis* recognized world-wide by the Integrated Taxonomic Information System (ITIS, www.ITIS.gov) and World Registry of Marine Species (WoRMS, www.marinespecies.org). The genus consists of prosobranch gastropods typified by ear-shaped shells that are pierced by several small spiracle holes. The shells are prized for their iridescent pearly appearance and have been used in jewelry, decorations, and even tools for millennia (Morris and others, 1980; Rick and others, 2002). The flesh of the large muscular foot also is considered to be a delicacy, and historically, abalone meat has commanded high prices. Though varying considerably in size, several of the California species are large for gastropods. Of the seven species, six were extensively fished, and although black abalone are considered inferior because of their tougher flesh, they sustained a recreational and commercial fishery until the 1990s. The annual commercial take for this species peaked in 1973 at about 873,000 kilograms (kg) or a little under 2-million pounds (California Department of Fish and Game, 2004).

The black abalone inhabits rocky shores from the high intertidal to a depth of approximately 6 meters (m), which is shallower than the other local species of the genus. Its range extends from Point Arena, California, to Isla de Cedros, Baja California Sur, Mexico, but it is most abundant from central California southward (VanBlaricom and others, 2009).

Smaller black abalone feed on diatom films and coralline algae, whereas larger individuals are thought to feed mainly on drift kelp (VanBlaricom and Kenner, 2020). The species can attain a shell length of up to 20 centimeters (cm). In addition to humans, natural predators of the black abalone include octopuses (*Octopus* spp.), sea stars (especially *Pisaster ochraceus*), cabezon (*Scorpaenichthys marmoratus*), and sea otters (*Enhydra lutris*; Morris and others, 1980).

The species is relatively sedentary, and some large specimens can go years without apparent movement. However, some of the few studies that have addressed movement in black abalone have reported that smaller individuals are more mobile and capable of movement on the order of several centimeters to a few meters in a day (VanBlaricom and others, 2009).

## Reproduction

Like many marine invertebrates, black abalone reproduce by broadcast spawning; a reproductive strategy in which mature male and female individuals release large numbers of gametes into the environment with no mutual physical contact necessary. Successful fertilization likely requires temporal synchrony and relatively close spatial proximity. Although several studies have concluded that black abalone populations spawn in late summer (Boolootian and others, 1962; Leighton and Boolootian, 1963; Webber and Giese, 1969), the actual trigger for spawning is unknown. In fact, unlike several other species of *Haliotis*, spawning of *H. cracherodii* in the laboratory has been met with limited success. Because the concentration of gametes in seawater is inversely related to the cube of the distance from their source, the proximity of spawning individuals is central to successful fertilization. Black abalone, as noted in the previous section, are somewhat sedentary and do not aggregate to spawn. There are many confounding factors to consider when attempting to calculate critical reproductive distance in intertidal organisms such as turbulence, channeling of water through crevices, and residency time of gametes in pools. It is likely though, that inter-abalone distances greater than a few meters resulted in reduced reproductive success compared with shorter distances (VanBlaricom and others, 2009), and average adult densities below 0.34 square meters ($m^2$) led to recruitment failure in some populations (Neuman and others, 2010). Abalone produce non-feeding larvae with a relatively short larval planktonic period. For this reason, bolstered by genetic evidence, it is thought that black abalone likely disperse relatively short distances (Chambers and others, 2006).

## Withering Syndrome

Withering syndrome (WS) is a disease that affects many species of *Haliotis* and results in atrophy of the "foot" and a diminished ability to cling to hard substrate. Animals showing signs of WS underwent body shrinkage as the disease progresses because of a combination of reduced food intake and changes in the structure of the digestive gland. The progressive degeneration eventually leads to death. The causative agent has been identified as a Rickettsiales-like prokaryotic organism (often referred to in the literature as "RLO"), specifically *Candidatus* Xenohaliotis californiensis (CaXc; Friedman and others, 2002). The disease was first observed in black abalone on the California Channel Islands. Beginning at Santa Cruz Island in 1985, it spread through the Channel Islands during the next few years, arriving at San Nicolas Island (SNI) in 1992 (Lafferty and Kuris, 1993; VanBlaricom and others, 1993). In black abalone populations afflicted with the disease, the mortality rate is typically at least 90 percent. Most southern California black abalone populations have been devastated by the disease which has since moved into central California populations, where it has caused significant levels of mortality (Miner and others, 2006). Although CaXc has been detected in black abalone throughout its range, populations north of San Luis Obispo County have not experienced the high levels of mortality associated with the disease in coastal areas to the south (National Marine Fisheries Service, 2020). Elevated water temperatures may accelerate disease transmission and mortality rates (Raimondi and others, 2002). Recent work has indicated that there is now genetic resistance to the WS infection in some black abalone populations on SNI. In addition, a viral bacteria-phage that infects CaXc could lend some protection (Friedman and others, 2014). It is too early to know how effective these factors will be in protecting wild populations.

The National Marine Fisheries Service (NMFS) listed *H. cracherodii* as an endangered species in January 2009. This action was taken to address concerns about the serial near-extinction of populations in southern California and Mexico, the continued movement of WS northward, and potential recruitment failures (74 FR 9, January 14, 2009; National Oceanic and Atmospheric Administration, 2009).

In their critical habitat designation for the black abalone, the NMFS excluded SNI because of revisions in the Navy's Integrated Natural Resource Management Plan (INRMP) that provide benefits to black abalone (76 FR 208, October 27, 2011; National Oceanic and Atmospheric Administration, 2011). One of the management strategies for marine invertebrates set forth in the INRMP was to "Promote and discuss current long-term monitoring of black abalone populations established in the late 1970s (VanBlaricom, 1993) and ensure that survey information on existing populations and trends are made available to the general scientific community" (U.S. Navy, 2015).

## Project History

The black abalone monitoring sites were established on SNI in 1980 (fig. 1) and first sampled in 1981 by Glenn VanBlaricom, then of the U.S. Fish and Wildlife Service. From 1981 to 1997, with a few exceptions, all sites were sampled during 10 cycles that each took 1 to 2 years to complete. Missed samples were as follows: transect 4 at site 7 was not sampled in cycle 1, transect 6 of site 1 and sites 3 and 8 was not sampled in cycle 2. Sampling was suspended during 1998–2000 because of an interruption in funding but resumed in 2001.

During the 1980s and 1990s, measurements of shell length were collected opportunistically. Samples of 100 or more abalone were measured during several cycles between 1983 and 1993, resulting in nearly 3,400 measurements made during 2 to 4 cycles at each site. On randomly selected transects at each site and beginning at a quadrat and direction that also were randomly chosen, all accessible abalone were measured until at least 100 animals were measured on the site.

Since the resumption of surveys in 2001, sampling of all sites has been completed every year, and all accessible abalone have been measured (or at least 200 per site where very numerous). The nearest neighbor distances for black abalone (distance to the closest conspecific) were measured consistently beginning in 2005. All sampling trips through 2017 were led by Glenn VanBlaricom. Monitoring cycles during 2018–21 were supported by the U.S. Navy and led by M.C. Kenner. The 2021 field season represented the 31st cycle of sampling the sites since they were established. A timeline of significant events is shown in figure 2.



**Figure 1.** Black abalone monitoring sites on San Nicolas Island, California, showing location, number of transects, and total sampling area at each site.

| Year | Cycle | |
|------|-------|---|
| 2021 | 31 | |
| 2020 | 30 | |
| 2019 | 29 | ← Estimation of recruit size class for non-measured abalone begins |
| 2018 | 28 | |
| 2017 | 27 | |
| 2016 | 26 | **Increasing recruitment and gradual population growth** |
| 2015 | 25 | |
| 2014 | 24 | |
| 2013 | 23 | |
| 2012 | 22 | |
| 2011 | 21 | |
| 2010 | 20 | |
| 2009 | 19 | |
| 2008 | 18 | |
| 2007 | 17 | |
| 2006 | 16 | |
| 2005 | 15 | ← Nearest neighbor measurements begin |
| 2004 | 14 | |
| 2003 | 13 | |
| 2002 | 12 | |
| 2001 | 11 | ← Black abalone sampling resumes with annual monitoring and regular shell length samples |
| 2000 | | |
| 1999 | | |
| 1998 | | |
| 1997 | 10 | **Population declines by approximately 99 percent** |
| 1996 | 9 | |
| 1995 | | |
| 1994 | | |
| 1993 | 8 | |
| 1992 | | ← Withering syndrome appears at SNI |
| 1991 | | |
| 1990 | 7 | |
| 1989 | | |
| 1988 | 6 | |
| 1987 | 5 | ← Sea otters reintroduced to SNI   **High density population dominated by large individuals** |
| 1986 | 4 | |
| 1985 | | |
| 1984 | 3 | |
| 1983 | | |
| 1982 | 2 | |
| 1981 | 1 | ← Sampling of black abalone sites begins |
| 1980 | | |

**Figure 2.**   Timeline of sampling cycles. Arrows indicate timing of major changes in sampling or changes in black abalone populations at San Nicolas Island, California. Bars along the line indicate cycles that occurred during a period longer than 1 year.

The original impetus for monitoring black abalone at SNI was the planned reintroduction of the southern sea otter (*Enhydra lutris nereis*), a top marine carnivore that feeds almost exclusively on shellfish. Although the southern sea otter historically occurred at SNI, it had been absent from the system for nearly a century because of overhunting. Between 1987 and 1990, 139 sea otters were translocated to SNI from the central California coast population (Rathbun and others, 2000). Sea otters, at northern locations, have substantially decreased subtidal red abalone populations, driving them below commercially viable levels (Watson, 2000). However, the potential effect of sea otter predation on intertidal black abalone populations was uncertain because they do not regularly use the intertidal zone for foraging (VanBlaricom, 1993).

During the first 10 years of monitoring, black abalone were very densely aggregated at the sites, with mean densities ranging from about 4 to 28 per m$^2$ and some 1-m$^2$ quadrats having more than 100 abalone stacked several deep. To what extent these densities were a natural or normal baseline, is debatable. Pressure from sea otter foraging was removed because of the otter population's extirpation by fur hunters in the 19th century. Even human harvest, that had been part of the system for millennia, was greatly reduced after the removal of indigenous people from SNI in 1835, and the establishment of active military control of the island in 1942 likely reduced access for most commercial and sport take.

Ironically, disease, rather than sea otter predation, caused the black abalone populations at SNI to decline. From the time WS appeared at SNI in 1992 until 2001, when regular annual sampling resumed, the population at these nine monitoring sites was reduced by more than 99 percent. The U.S. Geological Survey's intertidal monitoring sites on SNI, which use fixed quadrats not specifically targeting abalone, recorded a decline of similar magnitude during the same period (M.C. Kenner, U.S. Geological Survey, unpub. data, 2020).

# Methods

## Surveys

There are nine black abalone monitoring sites distributed around the island and each consists of two to seven permanent transects (fig. 1) that range in length from 7 to 40 m (table 1), depending on the availability of suitable habitat. These transects were established in areas that supported high densities of black abalone in 1980 and provide good coverage around the island. The transects are excellent for tracking trends but because they were not randomly placed, they cannot be used to estimate a more general population size or density. The transects are marked by multiple stainless-steel eyebolts, typically 5–10 m apart, that are epoxied into holes drilled in the substrate. During surveys, a meter tape is attached to the eyebolts and a 2-m-wide area centered on the transect is surveyed along the length of the transect. To provide better repeatability of effort and allow for finer scale data assessments, the belt transects are further divided into 1-$m^2$ quadrats on either side of the transect tape so that a 30-m transect has 60 quadrats and samples 60 $m^2$ of area. The only exceptions are at site 2 where transects 3 and 4 are treated as 1 m wide because the transect tapes there each run along a single crevice for their entire length. The total sampled area for all nine sites is 2,054 $m^2$. However, the actual surface area sampled is much greater because of the heterogeneity of the rocky shore including numerous crevices, ridges, and boulders.

**Table 1.**  Numbers of transects and their lengths and areas at each site, San Nicolas Island, California.

[Most transects are 2 meters (m) wide. Those marked with an asterisk (*) are 1 m wide (see "Methods" section). **Abbreviation**: $m^2$, square meter]

| Transect | Length (m) | Area ($m^2$) | Transect | Length (m) | Area ($m^2$) |
|---|---|---|---|---|---|
| Site 1 | | | Site 6 | | |
| 1 | 30 | 60 | 1 | 26 | 52 |
| 2 | 30 | 60 | 2 | 30 | 60 |
| 3 | 30 | 60 | 3 | 30 | 60 |
| 4 | 30 | 60 | 4 | 40 | 80 |
| 5 | 30 | 60 | Site 7 | | |
| 6 | 30 | 60 | 1 | 30 | 60 |
| Site 2 | | | 2 | 30 | 60 |
| 1 | 30 | 60 | 3 | 25 | 50 |
| 2 | 30 | 60 | 4 | 25 | 50 |
| *3 | 17 | 17 | 5 | 25 | 50 |
| *4 | 27 | 27 | Site 8 | | |
| 5 | 30 | 60 | 1 | 30 | 60 |
| 6 | 25 | 50 | 2 | 30 | 60 |
| Site 3 | | | 3 | 30 | 60 |
| 1 | 31 | 62 | 4 | 25 | 50 |
| 2 | 35 | 70 | 5 | 24 | 48 |
| 3 | 36 | 72 | Site 9 | | |
| 4 | 7 | 14 | 1 | 18 | 36 |
| 5 | 8 | 16 | 2 | 7 | 14 |
| 6 | 15 | 30 | 3 | 10 | 20 |
| 7 | 18 | 36 | 4 | 20 | 40 |
| Site 4 | | | 5 | 27 | 54 |
| 1 | 12 | 24 | 6 | 17 | 34 |
| 2 | 14 | 28 | | | |
| Site 5 | | | | | |
| 1 | 15 | 30 | | | |
| 2 | 12 | 24 | | | |
| 3 | 8 | 16 | | | |

Sampling cycles began on January 1, or sometimes in the last week of December, and in typical years, were completed during the winter, if possible, to take advantage of day-time negative low tides. This schedule was not possible in 2021, and sampling took place in late spring and early summer, often in the dark. The order in which sites were sampled was determined largely by tidal height and surf conditions.

Each quadrat was carefully searched for black abalone with the aid of handheld lights to assist searching cracks and crevices. If possible, the black abalone that were discovered were measured for maximum shell length with dividers to the nearest millimeter (fig. 3). Frequently, it was not possible to obtain a measurement because abalone often occur in crevices where they could not be reached or where measuring tools could not be used. The target sample size for shell measurements was at least 200 per site at sites where that many could be found. Beginning in sampling cycle 29 (2019), most inaccessible abalone and those met after the target number of measurements was reached at a site were assigned by visual estimation to one of two size bins: less than or equal 3 cm (recruit) or greater than 3 cm (non-recruit). This provided information that could be used in determining recruitment dynamics. In prior years, no effort was made to estimate size classes for unmeasured individuals. Although 3 cm represents an abalone that likely settled a year or more prior, it is considered here as a recruit into the counted population because smaller abalone are very cryptic and thus poorly represented in count data (National Marine Fisheries Service, 2020). At sites 7 and 8, where there were more than 200 abalone, the transects were sampled in the same order and from the same starting point each year to reduce temporal and observer sampling error in the size data. Since 2013, the actual number of abalone measured usually exceeded the target number at both these sites. At the remaining sites, transect sampling order was determined by field conditions.

For every black abalone on a transect, including non-measured individuals, the distance to the closest conspecific (nearest neighbor) was measured (or estimated) to the nearest centimeter; nearest neighbors were recorded even if they occurred outside of the transects. In addition, the microhabitat of each abalone was recorded as one of three classes: (1) open horizontal, (2) open vertical, or (3) crevice. The first two categories are characterized by open, non-cryptic habitats that are either less than or greater than a 45-degree angle from a horizontal plane. Crevice habitat consists of cracks, crevices, or pockets of any orientation. Additionally, the cover of exposed sand was estimated to the nearest 10 percent for each quadrat, and the presence and relative abundance of sea urchins in each quadrat and the radius length of all sea star species on the transects were recorded.

Unavoidably, counts were made with error because some abalone remained hidden in cryptic rock or biological refugia despite efforts to thoroughly search for them. In addition, surging water during unfavorable tides or surf events sometimes complicated field efforts.



**Figure 3.**    Shell length is measured to the nearest millimeter by using dividers and a ruler, San Nicolas Island, California. Photographs taken by M.C. Kenner, U.S. Geological Survey, January 22, 2019.

## Statistical Analysis

For each of the nine study sites and for the sum total of all sites combined, we summed abalone counts across transects and analyzed the respective time series for the recovery period from 2001, when the smallest number were counted, to 2021. We used generalized additive models (GAMs) to model the summed counts within each time series as randomly distributed observations around a smooth nonlinear function of year, and the variability of the counts around the smooth function were modeled as an overdispersed Poisson distribution (data dispersion beyond that expected from a Poisson model), or quasi-Poisson distribution. Each GAM function represents a process average that is the mean number of abalone on the surveyed transects aggregated at the site level, as a function of time around which the observed counts are distributed. The quasi-Poisson distribution was fitted by the "gam" function with a log link function from the "mgcv" package in R statistical software (https://www.r-project.org/), representing trends using a smooth spline function based on year (Hastie and Pregibon, 1992; R Core Team, 2017; Wood, 2017).

Following visually apparent inflexions in the GAM curve based on the total combined count from all the sites, the subperiods 2001–07, 2007–14, 2014–21 and the whole period from 2001 to 2021 were examined. Period percentage changes were calculated from the GAM-based estimates as follows:

$$\text{\% Change} = (N_2 - N_1) / N_1 \times 100\% \tag{1}$$

where

$N_1$     is the GAM-based estimate of mean number of abalone at the first year of a period, and

$N_2$     is the GAM-based estimate of mean number of abalone at the last year of a period.

Percent per annum changes also were calculated for each period from annualized rates of growth:

$$\text{\% Per Annum Change} = ((N_2 / N_1)^{1/y} - 1) \times 100\% \tag{2}$$

where

$N_1$     is the GAM-based estimate of mean number of abalone at the first year of a period,

$N_2$     is the GAM-based estimate of mean number of abalone at the last year of a period, and

$y$     is the number of years in the period of interest.

We calculated 95-percent confidence ranges for the percentage changes by first noting that GAM models with a log link function, as used with Poisson distributions, are analyzed on the log-scale before transforming its estimates back to original scale. We next note that the percentage change in equation 1 can be expressed in terms of $\log(N_1)$ and $\log(N_2)$ as follows, dropping the percentage notation for simplicity:

$$\text{Change} \ = \frac{N_2 - N_1}{N_1} = \frac{N_2}{N_1} - 1 =$$
$$\exp\left(\log\left(\frac{N_2}{N_1}\right)\right) - 1 \ = \ \exp(\log(N_2) - \log(N_1)) - 1 \tag{3}$$

Because of the flexible properties of GAM functions, we treated the estimates for $\log(N_1)$ and $\log(N_2)$ as independent and applied the variance formula for the difference of two independent variables, $\log(N_2) - \log(N_1)$, in other words, the sum $\text{Var}(\log(N_2)) + \text{Var}(\log(N_1))$. We then calculated the square root of this variance to derive the standard error and then calculated 95-percent confidence limits by adding and subtracting two standard errors from the log difference. Finally, we exponentiated the interval limits and subtracted one in accordance with equation 3 to obtain the 95-percent confidence range for the percentage change. We used similar methods to calculate the 95-percent confidence range for percent per annum change, except we used the following equation:

$$\text{Per Annum Change} = \exp((\log(N_2) - \log(N_1)) / y) - 1 \tag{4}$$

In the final transformation of the confidence range for percent per annum change, we divided the 95-percent confidence limits of the log difference by $y$ before exponentiating and subtracting one.

This approach results in symmetric confidence intervals on the log-scale, but after transformation the intervals are asymmetric on the original data scale. The asymmetry is to be expected because Poisson distributions and count distributions, in general, are skewed with longer tails to the right (toward higher values) compared to the left, which is bounded by 0. Furthermore, our approach to calculating confidence intervals for percent change is conservative because we treated the estimates at $N_1$ and $N_2$ as independent; therefore, our variance estimates for percent differences may be larger than true variability if the estimates are correlated.

## Sites

This section includes a brief description of the nine sites around the island. Refer to figure 1 for locations. Photographs of most of the transects, taken between 2016 and 2020, are in Kenner (2020).

Site 1 is in Bomber Cove on the north side of Vizcaino Point on SNI. There are six parallel 30-m transects arranged perpendicular to the shore within a 50-m-wide cove. Transect 1 follows along the base of a rock outcropping measuring several meters high. Transects 2–6 are on low bedrock with scattered boulders, approximately 0.25–0.75 m high. Surfgrass (*Phyllospadix* spp.), anemones (*Anthopleura* spp.), and purple urchins (*Strongylocentrotus purpuratus*) are common in the lower areas. The site is fairly exposed to the prevailing northwest swell.

Site 2 is in the Thousand Springs area on the northernmost point of the island. The six transects are scattered into three general areas with approximately 900 m between the westernmost and easternmost transects. Transects 1 and 2 parallel each other along pools on the main point near the range marker poles. Transects 3–5 are several hundred meters to the east in a combination of crevice (transects 3 and 4) and red algal clad boulder (transect 5) habitat. Transect 6, several hundred meters further to the east, runs along a broad flat bench with parallel pools and rockweed (*Silvetia compressa*) cover.

Site 3 spans approximately 1,600 m from transect 1, west to transect 7 in three areas along the northeast shore. Transects 1–3 parallel the shore along a narrow rocky bench at the base of a steep bank below the northwest end of the runway. Transects 1 and 3 are typically covered by the coralline algae (*Corallina vancouverensis*) and the red algae (*Mazzaella affinis*). However, transect 2 has been mostly bare since 2015, likely because of a sand burial event that eliminated abalone on transects 1 and 2. Transects 4–6 are clustered together on a fairly bare rock bench approximately 975 m to the west. Transect 7, another 640 m westward, is on a narrow *C. vancouverensis* covered rock ridge between a channel-like pool and the ocean.

Site 4, south of the east end sand spit, is the smallest of the sites. Although a challenge to access, site 4 consists of only two parallel transects a few meters apart, on a raised mussel (*Mytilus californianus*) covered intertidal bench separated from the shore.

Site 5, on the southeast shore of the island, has three transects parallel to shore spaced about 10 m apart. The transects are on slightly elevated, narrow reefs covered with *M. californianus*.

Site 6, near the old navigation light on the southeast shore of the island, consists of four transects spread out over about 300 m of shoreline. All the transects are on broad low relief reefs with *M. californianus* beds and some large patches of *Phyllospadix* spp.

Site 7, near the south side range marker poles, has five transects arranged upon one large rocky bench. Transect 1 is along the raised eastern edge of the reef. Transects 2 and 3

follow channels on top of the reef and intersect each other at about a 90-degree angle. Transects 4 and 5 are approximately 150 m west of transect 1 and traverse channels and crevices perpendicular to the shore in a jumbled, high relief area of the reef susceptible to sand incursion.

Site 8, on the southwest shore, is made up of five transects spread out over about 230 m of shoreline. Transect 1 parallels the shoreline on a low, flat ridge between two pools where a few boulders provide some cryptic habitat. Transects 2 and 3 are parallel to each other and the shoreline and follow low ridges with abundant crevice space. To the east, transects 4 and 5 also parallel each other but are perpendicular to the shoreline, traversing channels that are dominated by boulders and are susceptible to sand influence.

Site 9 is to the south of "Rock Crusher" on the west end of the island in an area fully exposed to the predominant westerly swells. Six transects are spread over approximately 170 m across an extensive low rock reef. The transects follow low ledges in an area with numerous boulders. *Corallina vancouverensis* and *Phyllospadix* spp. provide most of the cover.

## Results

Owing to the Coronavirus 2019 (Covid-19) outbreak, sampling during 2021 was delayed past the usual winter tide period and did not commence until late May, so the cycle 31 sampling of the sites took place between May 26 and July 10, 2021, and was spread out across three trips to the island. Because of this delay, unlike previous sampling cycles, virtually all the low tides were during the dark of night or early at dawn. Headlamps and work area lights were used in addition to the handheld flashlights. The times the sampling took place ranged from about 12:30 am to 9:30 am, Pacific Daylight Time. Generally, good conditions prevailed during the trips, with only a few days characterized by large surf.

### Counts

A total of 2,023 abalone were counted on all 9 sites in 2021 (2,054 m$^2$ sampled). This total was 318 fewer than were counted in 2020 but very similar to the 2019 count of 2,022. The total count represents a decline of 13.6 percent from counts made the previous year. Most of the decline occurred at site 8, where the highest numbers of abalone had been counted every year since 1996, a few years after WS appeared on SNI. The loss of 397 abalone from site 8 was a decline of 36.0 percent from the 2020 count at this site. Counts at five of the sites declined but increased at four.

Table 2 shows counts by transect at each site, the total count at each site, and the combined total for all sites for the last 5 years (2017–21). Transect 2 of site 8, which had the highest count every year since 2002, declined by 341 abalone (62.3 percent), which is more than the island-wide decrease in counted abalone in 2021. On the other 43 transects, changes in 2021 ranged from a decrease of 40 abalone to an increase of 42. The summed counts of abalone on these other transects increased by a total of 23 between 2020 and 2021. Of the 44 transects around the island, the counts of 22 transects declined, whereas 15 increased and 7 remained the same. The sites with the greatest increases in 2021 were site 1 (63), site 7 (44), and site 5 (24). Relative to the 2020 counts, site 1 increased by 80.7 percent and site 5 increased by 75.0 percent compared with just 6 percent for site 7. Like the 2020 increase at site 6, the 2021 increase at site 1 cannot be explained as a recruitment event owing to the low numbers of recruits detected there (5.0 percent) and must be the result of movement onto the transects from adjacent areas.

Zero abalone were counted on 6 of the 44 transects in 2021. For comparison, six transects in 2020 and five in 2019 had zero abalone counted. It is notable that transects 1 and 2 at site 3, which have had no abalone since a presumed sanding event occurred there in 2015, had small numbers of abalone on them in 2021 (three and four individuals respectively). Although two of these abalone were recruits, the others were adults that apparently immigrated on to the transects. In contrast, no abalone were counted on three transects that previously had small numbers on them: one transect at site 1 and two transects at site 9.

Figure 4 shows the combined total raw count from all the sites for each survey from 2001 to 2021, the calculated GAM curve, and the 95-percent confidence band (adjusted $R^2$=0.992). In the figure, the 2020 count seems anomalously high (above the calculated 95-percent confidence band around the calculated curve), but examination at the site level shows that the lower 2021 count resulted from the large reduction at site 8. Results at the other sites were mixed, with some increasing as much as 85 and others decreasing by as much as 31, but if not for the decline at site 8, there would have been a small net increase in the island count.

The whole island population trend during this period showed three general phases (table 3). During the initial 7 years, from 2001 to 2007, total black abalone counts underwent a relatively modest increase of 130 percent (15 percent per annum average). This modest increase was followed by a higher growth period from 2007 to 2014, with an increase of 290 percent (21 percent per annum average). Population growth was the most variable during the last phase, from 2014 to 2021, and overall growth declined to a slower rate, increasing only 25 percent (3 percent per annum average). During the period from 2001 to 2021, the population grew an average 13 percent per annum.

Figure 5 shows the logarithmic count trajectories, the calculated GAM curve, and the 95-percent confidence band for each of the sites. Population growth has been inconsistent among sites and over time since 2001. Although all sites showed positive growth during the period from 2001 to 2021, sites 3 and 8 experienced negative change during the period from 2014 to 2021 (table 3). Additionally, site 1 declined during the first period (2001–07) and site 5 declined during the second period (2007–14) when many sites had their highest population growth rate. Sites 2 and 9 had consistent average per annum rates of growth across the three periods of 17 and 11 percent, respectively. Site 5 had the lowest rate of growth during the period from 2001 to 2021, with an average per annum rate of 7 percent, whereas site 6 had the highest at 28 percent. Site 8, which accounts for more than one third of the surveyed population (largely because of the higher number of black abalone surviving there in 2001), had a very modest average per annum rate of increase from 2001 to 2021 (9 percent).

Figure 6 shows the counts at each of the sites during the project from 1981 to 2021. An inset graph of the last two decades with an expanded y-axis gives a better view of the recovery trends at the sites during this time.

Figure 7 shows how the counts at the different sites contributed to the total count from 2001 to 2021. During this time, site 8 had the highest count every year until 2021 when the count there declined by 36 percent. Site 7, which increased 6 percent in 2021, became the site with the highest black abalone counts. Although counts at site 6 declined by 7.1 percent, it remained third in abalone abundance.

Table 4 shows counts for each site during the course of the sampling program. Missing data from unsampled transects in the early 1980s (see the "Project History" section) were estimated for purposes of obtaining average pre-WS counts and densities and are noted in the table. Cycle 2 values were used as estimates for missing cycle 1 counts for transect 4 of site 7. Missing cycle 2 data for site 2, site 8 and transect 6 of site 1 were estimated by averaging the counts for those locations from cycle 1 and cycle 3. The average total count during the pre-WS period (1981–91) was 24,387 individuals. Although the count fell to 0.8 percent of that total in 2001, population growth occurred in most years during the next two decades. The 2021 total was 8.3 percent of the pre-WS average total. Mean densities at the sites, calculated as total site count per area surveyed, ranged from 4.0 to 27.8 per m$^2$ (11.9 per m$^2$ average) during the pre-WS period. In the 2021 field season, mean site densities ranged from 0.1 to 2.9 per m$^2$ with an average of 1.0 per m$^2$ (bottom green row in table 3). Unlike 2020, when all nine sites showed increases in total counts from the previous year, five of the sites declined in 2021, with changes ranging from a 40.3-percent decline to an 80.7-percent increase (blue row in table 3).

**Table 2.**    Number of black abalone counted on each site by transect, San Nicolas Island, California, 2017–21.

[Total count for each year is in bottom row.]

| Transect | Sample year (cycle) | | | | | Transect | Sample year (cycle) | | | | |
|---|---|---|---|---|---|---|---|---|---|---|---|
| | 2017 (27) | 2018 (28) | 2019 (29) | 2020 (30) | 2021 (31) | | 2017 (27) | 2018 (28) | 2019 (29) | 2020 (30) | 2021 (31) |
| Site 1 | | | | | | Site 6 | | | | | |
| 1 | 39 | 75 | 49 | 47 | 89 | 1 | 35 | 64 | 46 | 53 | 23 |
| 2 | 0 | 2 | 2 | 2 | 2 | 2 | 10 | 18 | 22 | 32 | 29 |
| 3 | 10 | 0 | 3 | 8 | 3 | 3 | 12 | 10 | 26 | 42 | 66 |
| 4 | 2 | 0 | 2 | 1 | 0 | 4 | 7 | 20 | 20 | 41 | 38 |
| 5 | 1 | 1 | 5 | 8 | 6 | All | 64 | 112 | 114 | 168 | 156 |
| 6 | 8 | 19 | 8 | 12 | 41 | Site 7 | | | | | |
| All | 60 | 97 | 69 | 78 | 141 | 1 | 199 | 216 | 217 | 180 | 188 |
| Site 2 | | | | | | 2 | 9 | 14 | 3 | 15 | 13 |
| 1 | 1 | 1 | 4 | 2 | 2 | 3 | 40 | 17 | 37 | 63 | 23 |
| 2 | 7 | 8 | 9 | 5 | 2 | 4 | 134 | 184 | 256 | 272 | 314 |
| 3 | 2 | 10 | 12 | 15 | 19 | 5 | 206 | 180 | 151 | 198 | 234 |
| 4 | 1 | 2 | 0 | 0 | 0 | All | 588 | 611 | 664 | 728 | 772 |
| 5 | 12 | 32 | 11 | 32 | 32 | Site 8 | | | | | |
| 6 | 0 | 0 | 0 | 0 | 0 | 1 | 252 | 111 | 58 | 42 | 18 |
| All | 23 | 53 | 36 | 54 | 55 | 2 | 476 | 524 | 625 | 547 | 206 |
| Site 3 | | | | | | 3 | 74 | 76 | 51 | 89 | 57 |
| 1 | 1 | 0 | 0 | 0 | 3 | 4 | 112 | 131 | 175 | 283 | 243 |
| 2 | 4 | 0 | 0 | 0 | 4 | 5 | 109 | 131 | 108 | 142 | 182 |
| 3 | 34 | 26 | 29 | 32 | 18 | All | 1,023 | 973 | 1,017 | 1,103 | 706 |
| 4 | 3 | 6 | 3 | 0 | 2 | Site 9 | | | | | |
| 5 | 1 | 3 | 1 | 1 | 1 | 1 | 6 | 2 | 1 | 9 | 2 |
| 6 | 1 | 0 | 2 | 2 | 1 | 2 | 3 | 3 | 6 | 9 | 7 |
| 7 | 14 | 14 | 7 | 12 | 14 | 3 | 2 | 0 | 0 | 0 | 0 |
| All | 58 | 49 | 42 | 47 | 43 | 4 | 3 | 3 | 3 | 6 | 0 |
| Site 4 | | | | | | 5 | 30 | 30 | 18 | 44 | 37 |
| 1 | 35 | 33 | 13 | 32 | 42 | 6 | 0 | 1 | 1 | 9 | 0 |
| 2 | 12 | 17 | 14 | 22 | 6 | All | 44 | 39 | 29 | 77 | 46 |
| All | 47 | 50 | 27 | 54 | 48 | All sites | | | | | |
| Site 5 | | | | | | All | 1,945 | 2,016 | 2,022 | 2,341 | 2,023 |
| 1 | 18 | 19 | 15 | 21 | 29 | | | | | | |
| 2 | 15 | 10 | 8 | 3 | 22 | | | | | | |
| 3 | 5 | 3 | 1 | 8 | 5 | | | | | | |
| All | 38 | 32 | 24 | 32 | 56 | | | | | | |
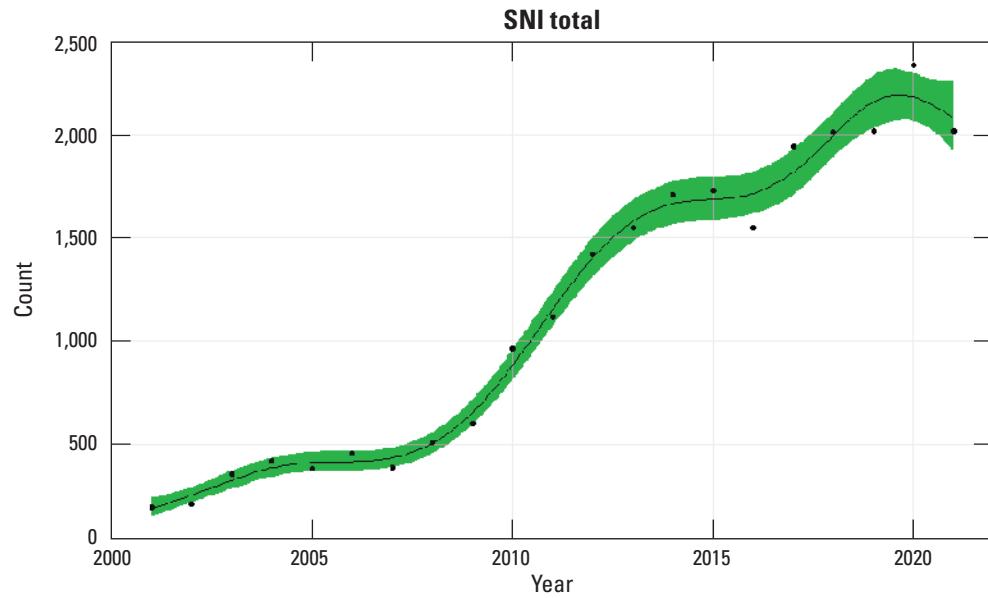
**Figure 4.** Total black abalone counts from all sites combined, generalized additive model nonlinear regression, and 95-percent confidence band, San Nicolas Island, California, 2001–21.

**Table 3.** Period (top) and per annum (bottom) percentage changes in mean black abalone counts during given periods calculated from general additive model (GAM) analysis, San Nicolas Island, California, 2001–21.

[Values in parenthesis () indicate 95-percent confidence range for GAM estimate each year.
**Abbreviation**: SNI, San Nicolas Island]

| Time frame | 2001–07 | 2007–14 | 2014–21 | 2001–21 |
|---|---|---|---|---|
| | | Site 1 | | |
| Period | −25 | 790 | 120 | 1,400 |
| | (−76–140) | (360–1,600) | (42–230) | (410–4,000) |
| Per annum | −5 | 37 | 12 | 14 |
| | (−21–16) | (24–50) | (5–19) | (9–20) |
| | | Site 2 | | |
| Period | 150 | 190 | 190 | 2,000 |
| | (18–440) | (84–360) | (110–320) | (970–4,200) |
| Per annum | 17 | 17 | 17 | 17 |
| | (3–32) | (9–25) | (11–23) | (13–21) |
| | | Site 3 | | |
| Period | 1,900 | 360 | −69 | 2,800 |
| | (170–5,000) | (180–650) | (−83–−42) | (270–22,000) |
| Per annum | 65 | 24 | −15 | 18 |
| | (18–130) | (16–33) | (−22–−7) | (7–31) |
| | | Site 4 | | |
| Period | 640 | 580 | 120 | 10,900 |
| | (13–4,730) | (200–1,300) | (34–260) | (1,700–66,000) |
| Per annum | 40 | 31 | 12 | 26 |
| | (2–91) | (18–46) | (4–20) | (17–38) |

**Table 3.**    Period (top) and per annum (bottom) percentage changes in mean black abalone counts during given periods calculated from general additive model (GAM) analysis, San Nicolas Island, California, 2001–21.—Continued

[Values in parenthesis () indicate 95-percent confidence range for GAM estimate each year.
**Abbreviation**: SNI, San Nicolas Island]

| Time frame | 2001–07 | 2007–14 | 2014–21 | 2001–21 |
|---|---|---|---|---|
| | | Site 5 | | |
| Period | 250 | −13 | 21 | 270 |
| | (60–680) | (−42–32) | (−30–110) | (56–800) |
| Per annum | 23 | −2 | 3 | 7 |
| | (8–41) | (−8–4) | (−5–11) | (2–12) |
| | | Site 6 | | |
| Period | 340 | 460 | 460 | 14,000 |
| | (110–830) | (260–790) | (330–640) | (7,100–27,000) |
| Per annum | 28 | 28 | 28 | 28 |
| | (13–45) | (20–37) | (23–33) | (24–32) |
| | | Site 7 | | |
| Period | 130 | 1,000 | 43 | 3,700 |
| | (12–390) | (720–1,400) | (20–70) | (1,800–7,400) |
| Per annum | 15 | 41 | 5 | 20 |
| | (2–30) | (35–48) | (3–8) | (16–24) |
| | | Site 8 | | |
| Period | 100 | 180 | −3 | 440 |
| | (49–180) | (140–220) | (−17–13) | (300–630) |
| Per annum | 13 | 16 | 0 | 9 |
| | (7–18) | (13–18) | (−3–2) | (7–10) |
| | | Site 9 | | |
| Period | 82 | 100 | 100 | 640 |
| | (7–210) | (45–180) | (47–180) | (340–1,200) |
| Per annum | 11 | 11 | 11 | 11 |
| | (1–21) | (5–16) | (6–16) | (8–13) |
| | | SNI total | | |
| Period | 130 | 290 | 25 | 1,000 |
| | (76–200) | (240–340) | (13–39) | (760–1,300) |
| Per annum | 15 | 21 | 3 | 13 |
| | (10–20) | (19–23) | (2–5) | (11–14) |
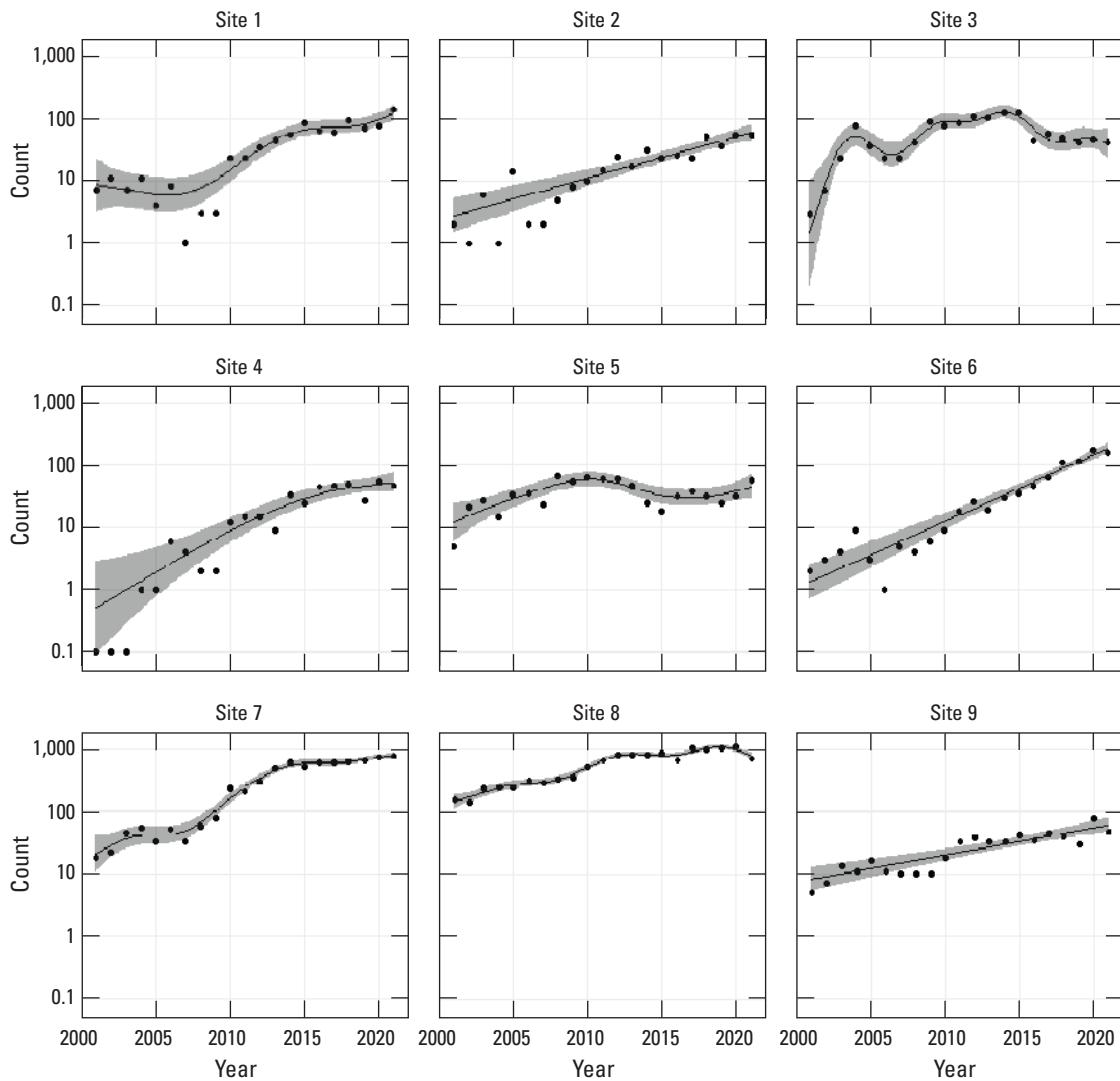
**Figure 5.**    Black abalone counts at each site at San Nicolas Island, California, plotted on a log scale, 2001–21. Curves and 95-percent confidence bands were generated by generalized additive model. (Zero values shown as 0.1 to allow plotting on the log-scaled axis).
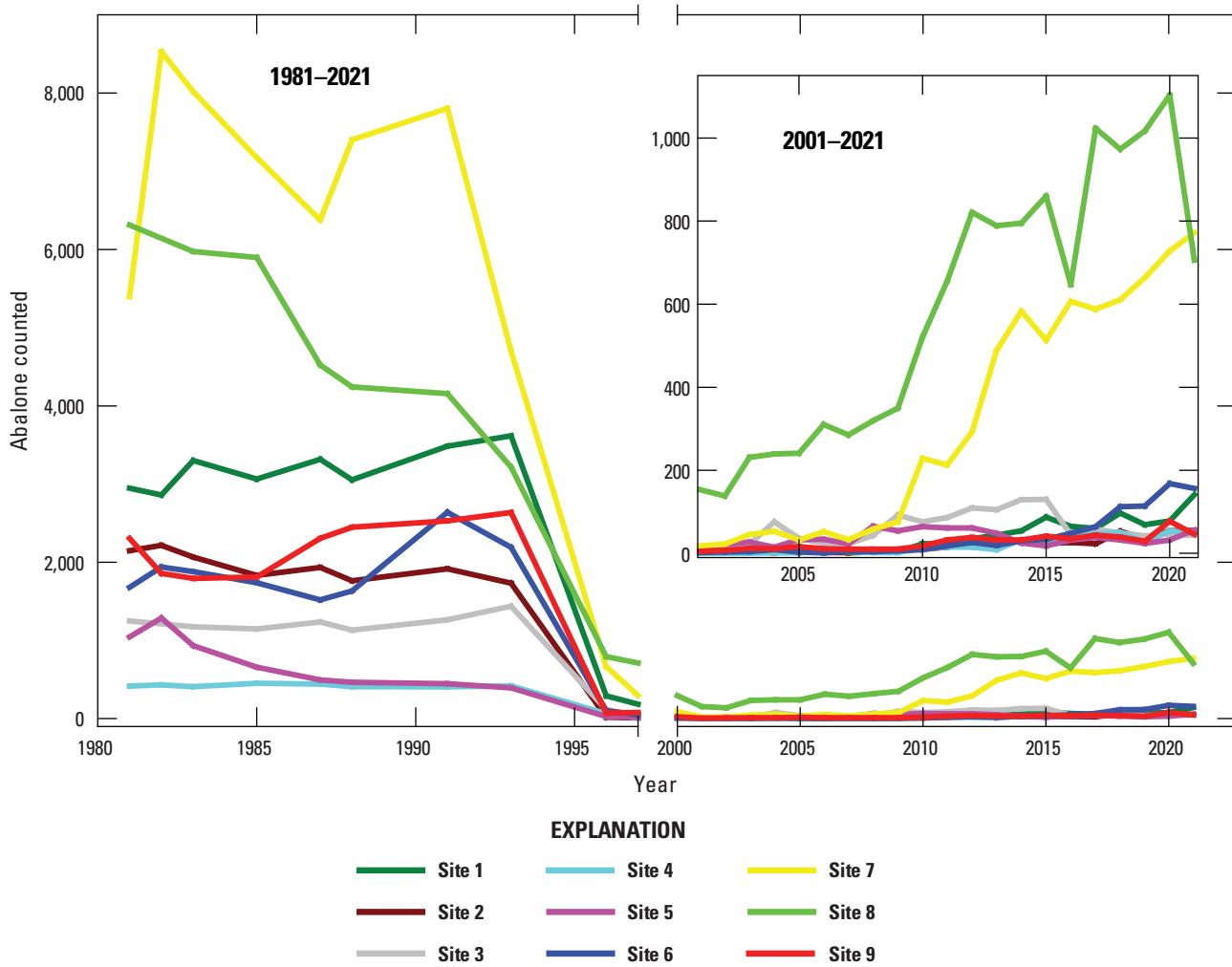
**Figure 6.**    Total black abalone count at each of the nine San Nicolas Island, California, sites during the study (1981–2021) and during the 2001–21 recovery phase after the withering syndrome outbreak (inset). No counts were made between 1997 and 2001.
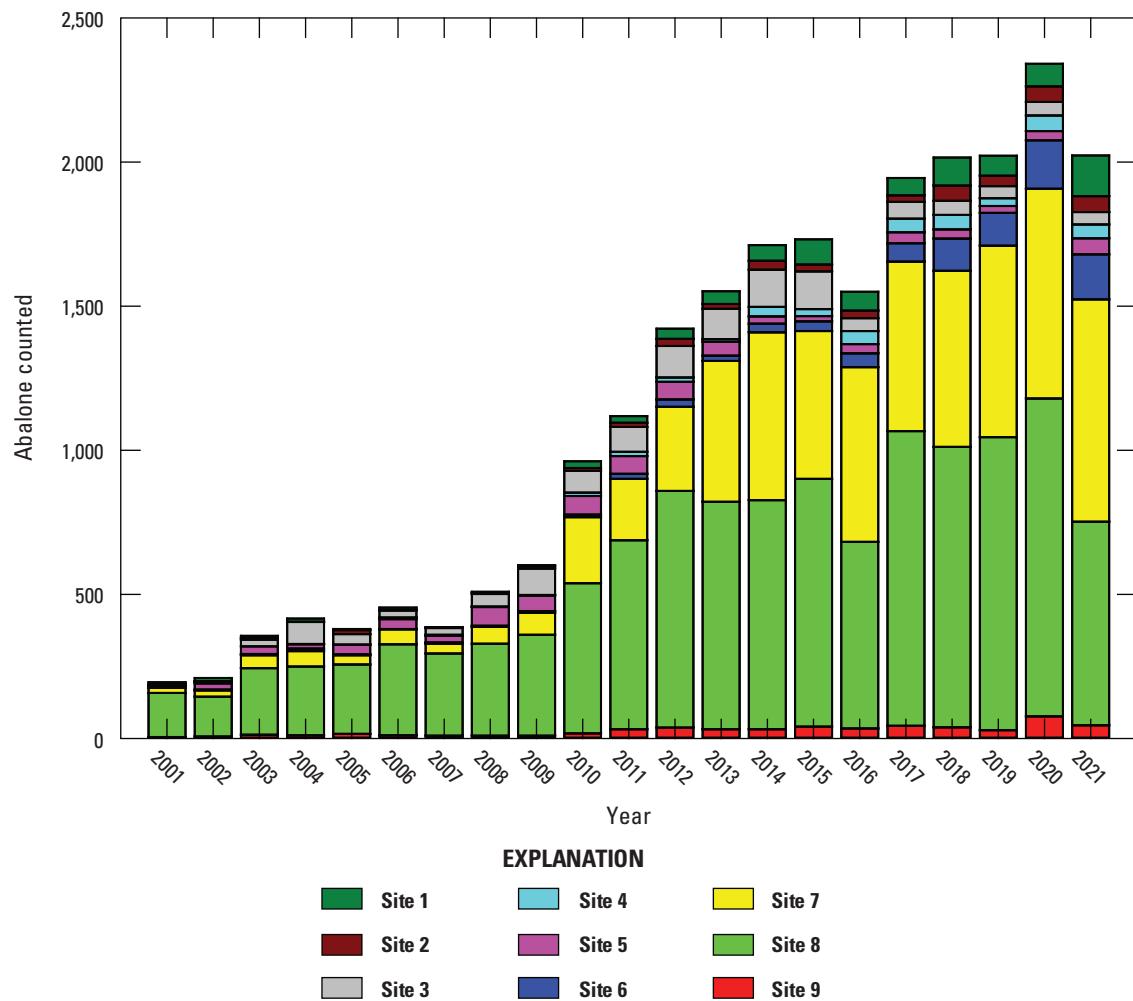
**Figure 7.**  Contribution of each site to total black abalone counts for 2001–21, San Nicolas Island, California.

**Table 4.**    Total black abalone counts by site for each sampling cycle, San Nicolas Island, California, 1981–2021.

[Far right column has cycle total. Average count and average density for pre-WS years shown after cycle 7. Percentage change from 2020 to 2021 and density in 2021 at each site and overall also shown. Asterisk (*) indicates some sites or transects were not sampled and total includes interpolated counts (see "Project History" section for details of missed counts). **Abbreviations**: —, not applicable; m², square meter]

| Cycle | Year completed | Site 1 | Site 2 | Site 3 | Site 4 | Site 5 | Site 6 | Site 7 | Site 8 | Site 9 | Cycle total |
|---|---|---|---|---|---|---|---|---|---|---|---|
| 1 | 1981 | 2,946 | 2,146 | 1,247 | 415 | 1,044 | 1,677 | *7,138 | 6,313 | 2,304 | *25,230 |
| 2 | 1982 | *3,227 | 2,215 | *1,210 | 431 | 1,286 | 1,938 | 8,531 | *6,144 | 1,856 | *26,838 |
| 3 | 1983 | 3,300 | 2,065 | 1,174 | 408 | 933 | 1,880 | 8,019 | 5,975 | 1,792 | 25,546 |
| 4 | 1985 | 3,062 | 1,830 | 1,147 | 450 | 657 | 1,737 | 7,177 | 5,899 | 1,811 | 23,770 |
| 5 | 1987 | 3,314 | 1,933 | 1,235 | 442 | 495 | 1,517 | 6,377 | 4,523 | 2,303 | 22,139 |
| 6 | 1988 | 3,053 | 1,763 | 1,131 | 407 | 465 | 1,631 | 7,403 | 4,245 | 2,446 | 22,544 |
| 7 | 1991 | 3,482 | 1,916 | 1,263 | 405 | 446 | 2,638 | 7,806 | 4,158 | 2,528 | 24,642 |
| Average count for cycles 1–7 | | | | | | | | | | | |
| — | — | 3,197.7 | 1,981.1 | 1,201.0 | 422.6 | 760.9 | 1,859.7 | 7,493.0 | 5,322.4 | 2,148.6 | 24,387.0 |
| Average density per m² for cycles 1–7 | | | | | | | | | | | |
| — | — | 8.9 | 7.2 | 4.0 | 8.1 | 10.9 | 7.4 | 27.8 | 19.2 | 10.9 | 11.9 |
| 8 | 1993 | 3,616 | 1,731 | 1,435 | 417 | 392 | 2,190 | 4,702 | 3,216 | 2,635 | 20,334 |
| 9 | 1996 | 290 | 18 | 115 | 63 | 26 | 102 | 666 | 792 | 72 | 2,144 |
| 10 | 1997 | 183 | 8 | 21 | 6 | 17 | 48 | 297 | 712 | 78 | 1,370 |
| 11 | 2001 | 7 | 2 | 3 | 0 | 5 | 2 | 18 | 153 | 5 | 195 |
| 12 | 2002 | 11 | 1 | 7 | 0 | 21 | 3 | 22 | 138 | 7 | 210 |
| 13 | 2003 | 7 | 6 | 22 | 0 | 27 | 4 | 45 | 231 | 12 | 354 |
| 14 | 2004 | 11 | 1 | 76 | 1 | 15 | 9 | 53 | 239 | 11 | 416 |
| 15 | 2005 | 4 | 14 | 36 | 1 | 33 | 3 | 32 | 241 | 16 | 380 |
| 16 | 2006 | 8 | 2 | 24 | 6 | 34 | 1 | 52 | 310 | 11 | 448 |
| 17 | 2007 | 1 | 2 | 23 | 4 | 23 | 5 | 30 | 285 | 10 | 383 |
| 18 | 2008 | 3 | 5 | 43 | 2 | 65 | 4 | 58 | 319 | 10 | 509 |
| 19 | 2009 | 3 | 8 | 92 | 2 | 54 | 6 | 76 | 352 | 10 | 603 |
| 20 | 2010 | 23 | 10 | 76 | 12 | 64 | 9 | 229 | 521 | 18 | 962 |
| 21 | 2011 | 23 | 15 | 86 | 15 | 61 | 18 | 213 | 656 | 32 | 1,119 |
| 22 | 2012 | 35 | 25 | 109 | 15 | 61 | 26 | 307 | 821 | 38 | 1,437 |
| 23 | 2013 | 44 | 17 | 105 | 9 | 48 | 19 | 489 | 789 | 32 | 1,552 |
| 24 | 2014 | 54 | 31 | 129 | 33 | 25 | 30 | 583 | 795 | 32 | 1,712 |
| 25 | 2015 | 87 | 24 | 130 | 24 | 18 | 34 | 513 | 860 | 41 | 1,731 |
| 26 | 2016 | 65 | 26 | 45 | 45 | 32 | 48 | 607 | 647 | 35 | 1,550 |
| 27 | 2017 | 60 | 23 | 58 | 47 | 38 | 64 | 588 | 1,023 | 44 | 1,945 |
| 28 | 2018 | 97 | 53 | 49 | 50 | 32 | 112 | 611 | 973 | 39 | 2,016 |
| 29 | 2019 | 69 | 36 | 42 | 27 | 24 | 114 | 664 | 1,017 | 29 | 2,022 |
| 30 | 2020 | 78 | 54 | 47 | 54 | 32 | 168 | 728 | 1,103 | 77 | 2,341 |
| 31 | 2021 | 141 | 55 | 43 | 48 | 56 | 156 | 772 | 706 | 46 | 2,023 |
| Percentage change from 2020 to 2021 | | | | | | | | | | | |
| — | — | 80.7 | 1.9 | −8.5 | −11.1 | 75.0 | −7.1 | 6.0 | −36.0 | −40.3 | −13.6 |
| Density per m² in 2021 | | | | | | | | | | | |
| — | — | 0.4 | 0.2 | 0.1 | 1.0 | 0.8 | 0.6 | 2.9 | 2.5 | 0.2 | 1.0 |

Figures 8 and 9 show how the counted abalone were distributed along each transect on sites 7 and 8, the two sites with the most abalone, during the most recent 5-year period (2017–21). Generally, abalone on the transects had a clumped distribution. In 2021, the highest 1-m² quadrat count was 61 abalone compared to 69 in 2020 and 74 in 2019. Of the 2,054 total 1-m² quadrats at all sites, the number of quadrats having zero abalone increased to 1,698 in 2021 from 1,649 in 2020. There were 1,735 quadrats with zero abalone in 2019. There was no change in the count in 1,532 quadrats but 208 quadrats increased and 271 decreased. Of the 356 quadrats that had abalone in 2021, 43 had the same number as in 2020. Of the 313 quadrats that did change, 208 increased compared to 105 that decreased. More than 75 percent of those that changed did so by 5 abalone or less, but differences ranged from an increase of 39 abalone to a decrease of 52.

Abalone were most commonly observed in the crevice microhabitat. Between 1983, when microhabitat was first recorded, and 1993, an average 65.9 percent of sampled abalone were in the crevice microhabitat category. In surveys completed between 2001 and 2021, after the WS induced population decline, the average rose to 95.0 percent. In 2021, 92.5 percent of abalone recorded were in the crevice microhabitat. Table 5 shows the number of abalone by microhabitat categories at the sites in 2021. The only transects where most abalone were not in crevice habitat were at site 6, the site with the least amount of relief and complexity. On 2 of the 4 transects at that site, open habitat was used by 60.1 and 72.4 percent of the abalone. Overall, at site 6, 30.1 percent of abalone occurred in open habitats in 2021.

## Size Distribution and Recruitment

Before WS reached SNI in the early 1990s, the size distribution of black abalone at these sites was dominated by large adults (VanBlaricom, 1993). During 2001–21, the period after WS dramatically reduced the population, recruits, here defined as abalone 3 cm or less in shell length, began to become more common (fig. 10). This phenomenon, in concert with the dramatic reduction of the existing population, led to a change in the overall shape of the size distribution. Of the 3,971 abalone measured before 1994, only 18 were in the recruit size class (0.45 percent), and none of the samples from a site contained more than 4 percent recruits. The low level of recruits recorded during that period contrasts with the size distributions from 2001 to 2021 when the percentage of recruits among all the abalone measured only fell below 4 percent a few times and in the samples after 2009, recruits often made up more than 10 percent of the measured total.

In 1988 (cycle 6), approximately 100 shell lengths were measured from each of the 9 sites (G.R. VanBlaricom, U.S. Geological Survey, unpub. data, 2019) and those data are used in this report for comparison with the more recent length distributions of the samples made since 2001. Because many of the recorded abalone could not be measured, there

likely is some bias in the length data from the pre-WS years. The very high densities of adults at the time could have made juveniles and small recruits more difficult to see. This bias likely changed over time as abalone became much less abundant and crowded. The potential for bias in the counts and measurements made at the different sites and transects likely varied also because of local topography. In the data for cycle 6, before the onset of WS, most individuals had shell lengths of 10–13 cm (fig. 11). Proportionately, there were very few individuals in the recruit size class—and few small individuals in general. This lack of recruits contrasts with the size distributions from 2001 onward (fig. 11). The size classes are much more evenly represented in the later years. Moreover, several of the recent years were dominated by smaller size classes. All these samples show at least a few individuals in the recruitment size class. In their first year, recently settled abalone are thought to primarily inhabit cryptic habitat such as *Mytilus* beds or under boulders. As a result, individuals less than 2 or 3 cm likely are under-represented in size samples (VanBlaricom, 1993). The percent of the sample that is made up of these less than 3.1 cm individuals is noted on each of the annual size plots in figure 11 and was as high as 26.5 percent in 2017.

The size frequency for each of the nine sites in 2020 and in 2021 is illustrated in figure 12. All nine sites had some individuals in the recruitment cohort in 2020, whereas six of the nine had some in 2021. Sites 7 and 8 had the most individuals in this category in both years, but as a percentage of the local population, sites 3 and 5 had the highest percentages. Site 8 had the most individuals larger than 15 cm. Table 6 shows numbers of recruits by site for each year from 2001 to 2021. Sites 7 and 8 generally had the most recruits after 2009.

A strong recruitment event was detected at site 8, transects 1 and 2, in 2017. Figure 13 illustrates the sequence of size frequencies on these transects from 2016 to 2021. Note that the frequencies plotted are numbers of individuals rather than percentage of the sample and only represents the part of the population on the transects that was measured, but the total number counted is indicated on the figure. Although the recruitment observed on transect 1 in 2017 increased total counts from 14 to 252, there was only a net gain of 4 individuals (from 14 to 18) by 2021, even though there were additional recruits in subsequent years. The total number of recruits measured on transect 1 from 2017 to 2021 was 247. On transect 2, total counts increased from 332 to 625 in 2019 but by 2021, despite the addition of 222 more measured or estimated recruits, the total count on the transect fell to 206, which is 126 less than it was in 2016.

A comparison of the shell lengths measured on site 8, transect 2 in 2020 and 2021 indicates that most of the loss between years was made up of individuals measuring 10 cm or less (fig. 14). Some of the largest declines between these years were in the young but mature segment of the population in the 5–10 cm size range.
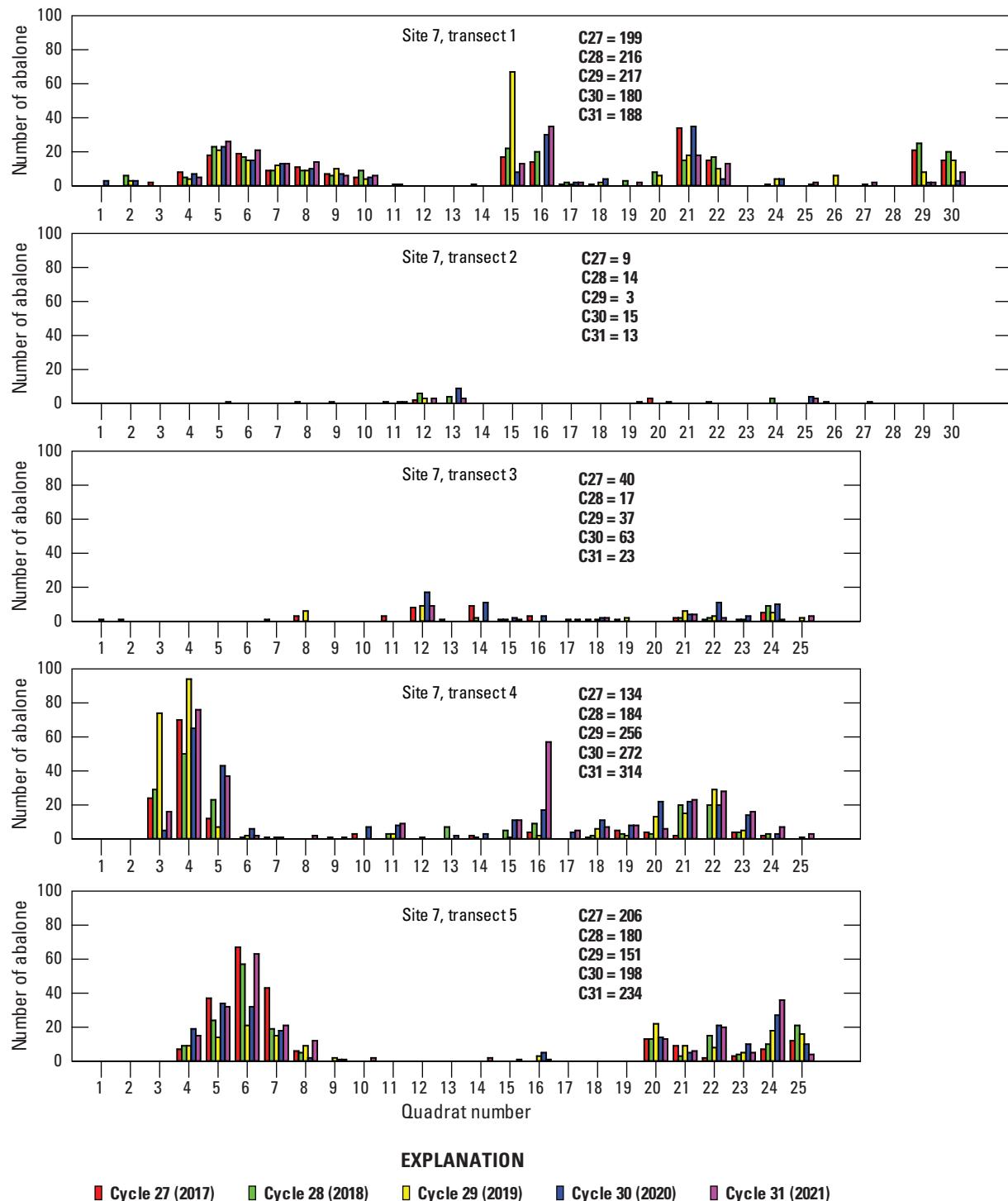
**Figure 8.**    Distribution of black abalone along each transect at site 7, San Nicolas Island, California, 2017–21. The total transect count for each cycle is indicated on graph. Quadrat totals are for the left and right sides of the transect combined (2 square meters).
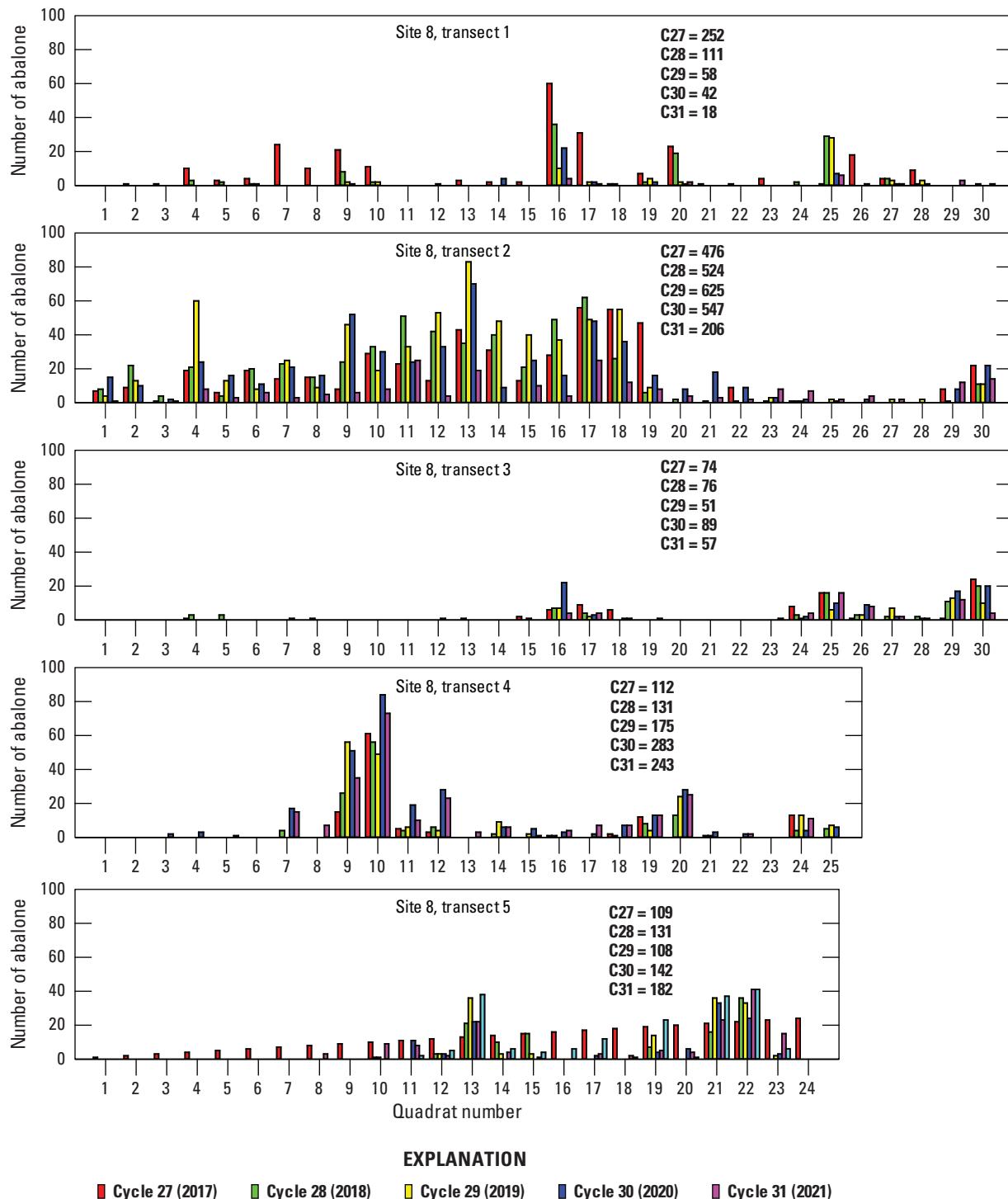
**Figure 9.** Distribution of black abalone along each transect at site 8, San Nicolas Island, California, 2017–21. The total transect count for each cycle is indicated on graph. Quadrat totals are for the left and right sides of the transect combined (2 square meters).

**Table 5.**    Number of abalone in each microhabitat by site and transect, San Nicolas Island, California, 2021.

[Percentage of abalone on each transect that were in crevice microhabitat is noted and shown with an asterisk (*) if less than 90 percent. Transects with no abalone counted are not listed]

| Transect | Crevice | Open horizontal | Open vertical | Percent crevice | Transect | Crevice | Open horizontal | Open vertical | Percent crevice |
|---|---|---|---|---|---|---|---|---|---|
| Site 1 | | | | | Site 6 | | | | |
| 1 | 89 | 0 | 0 | 100.0 | 1 | 9 | 14 | 0 | *39.1 |
| 2 | 2 | 0 | 0 | 100.0 | 2 | 8 | 21 | 0 | *27.6 |
| 3 | 3 | 0 | 0 | 100.0 | 3 | 59 | 0 | 7 | *89.4 |
| 5 | 6 | 0 | 0 | 100.0 | 4 | 33 | 4 | 1 | *86.8 |
| 6 | 41 | 0 | 0 | 100.0 | Site 7 | | | | |
| Site 2 | | | | | 1 | 186 | 0 | 2 | 98.9 |
| 1 | 2 | 0 | 0 | 100.0 | 2 | 12 | 1 | 0 | 92.3 |
| 2 | 2 | 0 | 0 | 100.0 | 3 | 18 | 3 | 2 | *78.2 |
| 3 | 19 | 0 | 0 | 100.0 | 4 | 311 | 1 | 2 | 99.0 |
| 5 | 32 | 0 | 0 | 100.0 | 5 | 219 | 0 | 15 | 93.6 |
| Site 3 | | | | | Site 8 | | | | |
| 1 | 3 | 0 | 0 | 100.0 | 1 | 15 | 1 | 2 | *83.3 |
| 2 | 4 | 0 | 0 | 100.0 | 2 | 169 | 31 | 6 | *82.0 |
| 3 | 18 | 0 | 0 | 100.0 | 3 | 38 | 19 | 0 | *66.7 |
| 4 | 2 | 0 | 0 | 100.0 | 4 | 243 | 0 | 0 | 100.0 |
| 5 | 1 | 0 | 0 | 100.0 | 5 | 177 | 0 | 5 | 97.3 |
| 6 | 1 | 0 | 0 | 100.0 | Site 9 | | | | |
| 7 | 14 | 0 | 0 | 100.0 | 1 | 2 | 0 | 0 | 100.0 |
| Site 4 | | | | | 2 | 7 | 0 | 0 | 100.0 |
| 1 | 31 | 11 | 0 | *73.8 | 5 | 37 | 0 | 0 | 100.0 |
| 2 | 5 | 1 | 0 | *83.3 | | | | | |
| Site 5 | | | | | | | | | |
| 1 | 26 | 1 | 0 | 96.3 | | | | | |
| 2 | 22 | 0 | 0 | 100.0 | | | | | |
| 3 | 5 | 0 | 0 | 100.0 | | | | | |

**Figure 10.**    Two black abalone recruits at site 5—Shell length approximately 2 centimeters (cm) in abandoned urchin cavities, San Nicolas Island, California. Photograph taken by M.C. Kenner, U.S. Geological Survey.
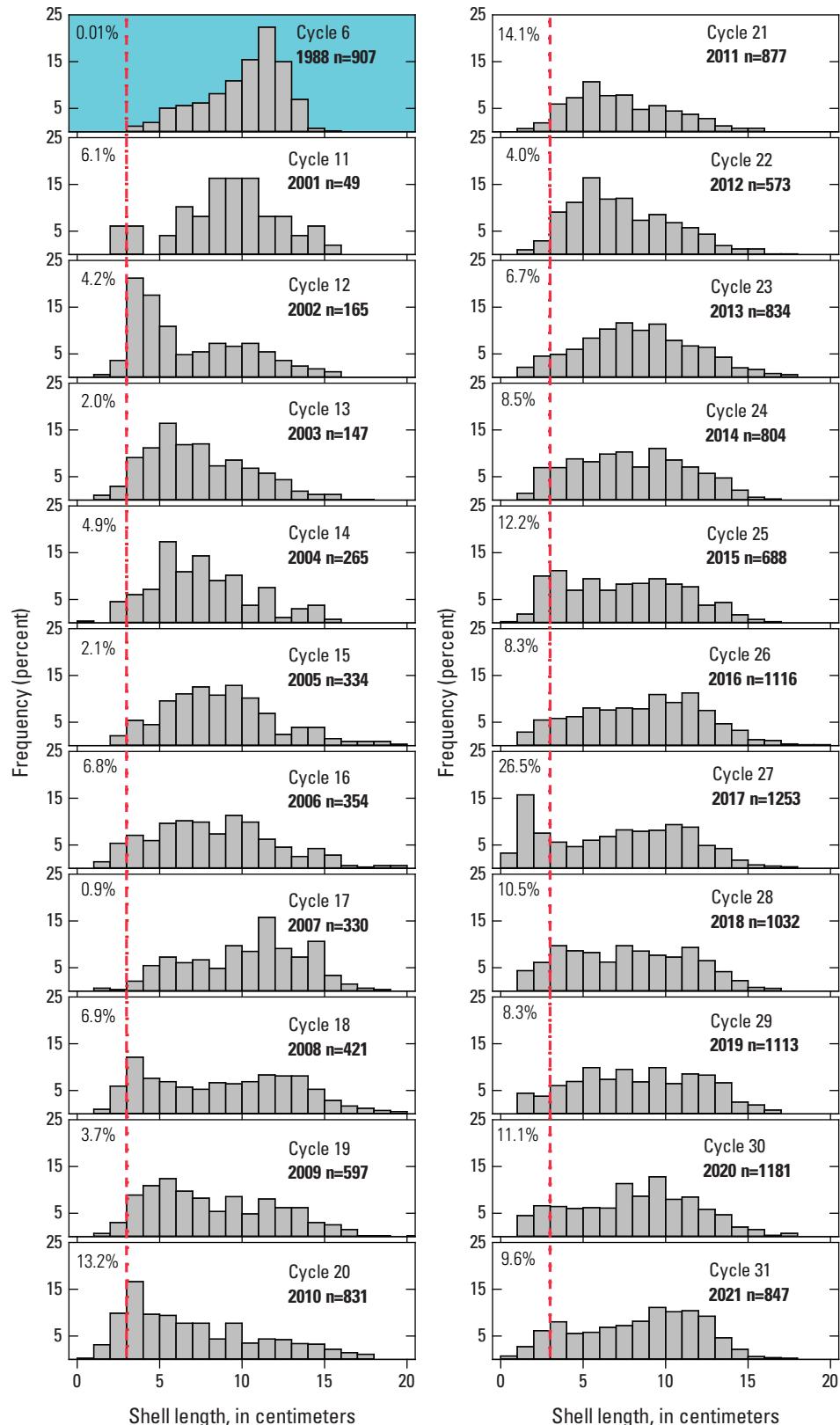
**Figure 11.**    Whole island size distributions (total shell length in centimeters) of black abalone for 1988 (colored background) and 2001–21, San Nicolas Island, California. Sizes to the left of the dashed red line are considered recruits and the percentage of each sample in that category is indicated.
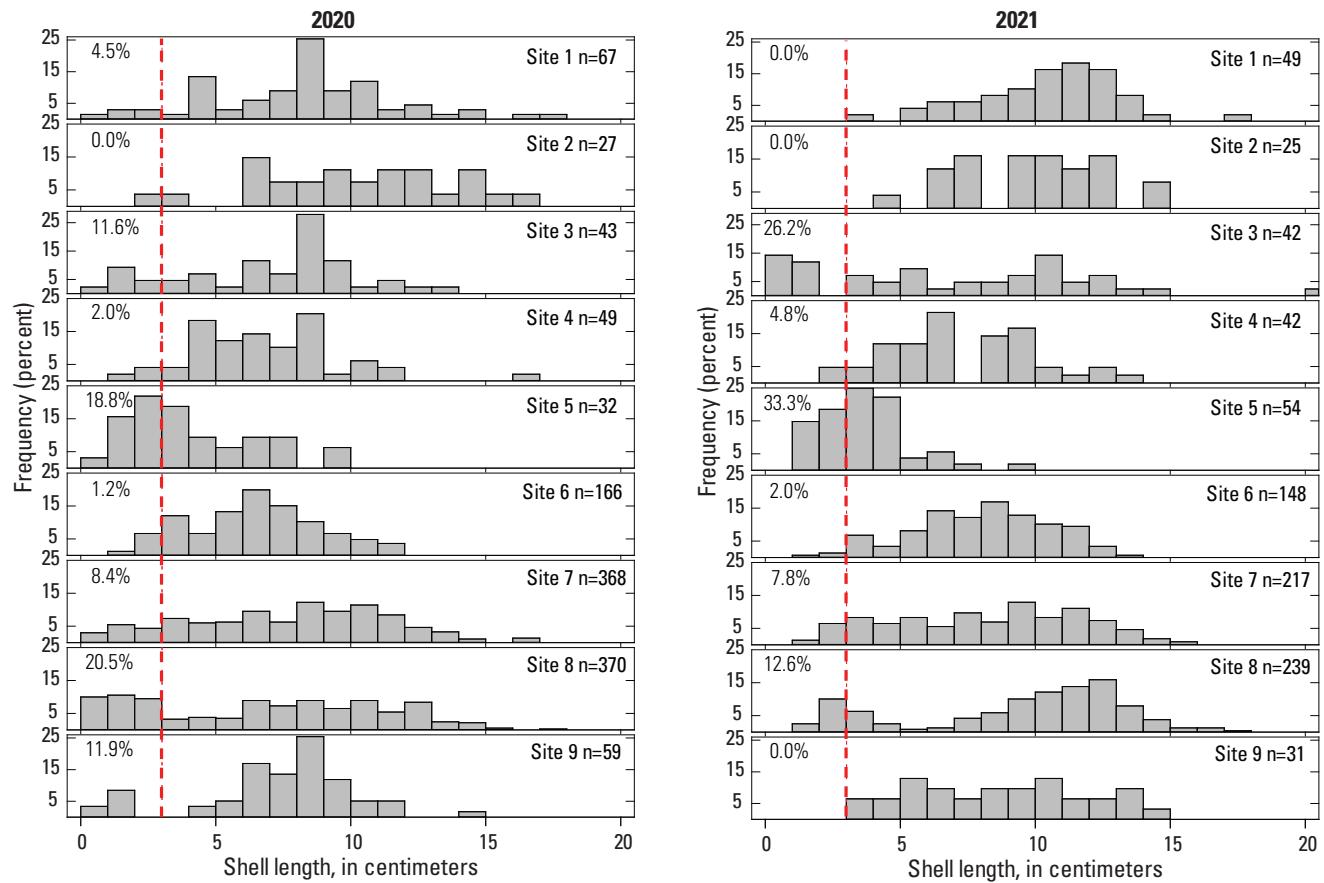
**Figure 12.** Size distribution (percentage frequency) of each site in 2020 (left) and 2021 (right), San Nicolas Island, California. Sizes to the left of the dashed red line are considered recruits and the percentage of each sample in that category is indicated.

**Table 6.** Number and percentage of measured abalone at each site that were recruits (less than 3.1 centimeters) for cycles 11–31 (2001–21) and total recruits for each cycle, San Nicolas Island, California.

[Values in parenthesis ( ) indicate percent. Bottom rows show numbers of non-measured abalone estimated to be in the recruit size bin in cycle 29, 30, and 31, and as a percentage of sized abalone—either measured or estimated into size bins—for those cycles (see "Methods" section). **Abbreviation**: NR, not recorded]

| Cycle | Year | Site | | | | | | | | | All sites |
| --- | --- | --- | --- | --- | --- | --- | --- | --- | --- | --- | --- |
| | | 1 | 2 | 3 | 4 | 5 | 6 | 7 | 8 | 9 | |
| 11 | 2001 | 0 | 0 | 0 | 0 | 0 | 0 | 0 | 3 | 0 | 3 |
| | | | | | | | | | (8.3) | | (5.5) |
| 12 | 2002 | 1 | 0 | 0 | 0 | 0 | 0 | 0 | 6 | 0 | 7 |
| | | (10.1) | | | | | | | (6.1) | | (4.2) |
| 13 | 2003 | 0 | 0 | 2 | 0 | 1 | 0 | 0 | 0 | 0 | 3 |
| | | | | (11.8) | | (8.0) | | | | | (1.9) |
| 14 | 2004 | 0 | 0 | 3 | 0 | 0 | 0 | 3 | 7 | 0 | 13 |
| | | | | (5.9) | | | | (7.0) | (5.4) | | (4.9) |
| 15 | 2005 | 0 | 0 | 1 | 0 | 3 | 0 | 0 | 3 | 0 | 7 |
| | | | | (2.8) | | (10.3) | | | (1.5) | | (2.1) |
| 16 | 2006 | 0 | 0 | 2 | 0 | 8 | 0 | 1 | 13 | 0 | 24 |
| | | | | (8.3) | | (23.5) | | (2.0) | (5.9) | | (6.8) |
| 17 | 2007 | 0 | 0 | 1 | 0 | 0 | 0 | 0 | 2 | 0 | 3 |
| | | | | (5.3) | | | | | (0.8) | | (0.9) |
| 18 | 2008 | 0 | 0 | 9 | 0 | 8 | 0 | 1 | 11 | 0 | 29 |
| | | | | (21.4) | | (12.3) | | (2.1) | (4.5) | | (6.8) |
| 19 | 2009 | 0 | 1 | 6 | 0 | 9 | 0 | 1 | 5 | 0 | 22 |
| | | | (12.5) | (6.6) | | (16.7) | | (1.4) | (1.4) | | (3.7) |
| 20 | 2010 | 2 | 2 | 9 | 2 | 13 | 0 | 31 | 51 | 0 | 131 |
| | | (9.5) | (20.0) | (13.2) | (16.7) | (21.7) | | (18.1) | (11.0) | | (15.8) |
| 21 | 2011 | 2 | 4 | 7 | 1 | 9 | 0 | 14 | 85 | 2 | 124 |
| | | (8.7) | (26.7 | (9.2) | (6.7) | (15.8) | | (9.3) | (17.2) | (7.4) | (14.1) |
| 22 | 2012 | 1 | 2 | 1 | 0 | 5 | 0 | 8 | 5 | 1 | 23 |
| | | (5.0) | (8.3) | (1.3) | | (8.8) | | (3.9) | (3.7) | (3.4) | (4.0) |
| 23 | 2013 | 0 | 0 | 6 | 0 | 12 | 0 | 35 | 3 | 0 | 56 |
| | | | | (6.6) | | (30.0) | | (9.6) | (1.2) | | (6.7) |
| 24 | 2014 | 3 | 3 | 8 | 2 | 6 | 0 | 23 | 23 | 0 | 68 |
| | | (7.5) | (14.3) | (11.1) | (6.1) | (25.0) | | (6.3) | (11.6) | | (8.5) |
| 25 | 2015 | 0 | 1 | 16 | 0 | 6 | 1 | 30 | 29 | 1 | 84 |
| | | | (4.5) | (17.0) | | (37.5) | (3.2) | (14.0) | (14.3) | (3.1) | (12.2) |
| 26 | 2016 | 3 | 6 | 0 | 0 | 4 | 3 | 60 | 9 | 8 | 93 |
| | | (8.3) | (26.1) | | | (16.7) | (6.5) | (15.4) | (1.7) | (26.7) | (8.3) |
| 27 | 2017 | 12 | 0 | 8 | 3 | 10 | 5 | 31 | 245 | 18 | 332 |
| | | (28.6) | | (14.3) | (6.4) | (31.3) | (8.5) | (15.1) | (30.5) | (40.9) | (26.5) |
| 28 | 2018 | 3 | 0 | 1 | 0 | 1 | 3 | 14 | 86 | 0 | 108 |
| | | (4.7) | | (2.1) | | (3.2) | (2.8) | (6.7) | (18.5) | | (10.5) |
| 29 | 2019 | 3 | 2 | 0 | 0 | 1 | 0 | 13 | 70 | 3 | 92 |
| | | (6.8) | (8.0) | | | (4.3) | | (4.0) | (13.4) | (12.5) | (8.3) |
| 30 | 2020 | 3 | 0 | 5 | 1 | 6 | 2 | 31 | 76 | 7 | 131 |
| | | (4.5) | | (11.6) | (2.0) | (18.8) | (1.2) | (8.4) | (20.5) | (11.9) | (11.1) |

**Table 6.** Number and percentage of measured abalone at each site that were recruits (less than 3.1 centimeters) for cycles 11–31 (2001–21) and total recruits for each cycle, San Nicolas Island, California.—Continued

[Values in parenthesis ( ) indicate percent. Bottom rows show numbers of non-measured abalone estimated to be in the recruit size bin in cycle 29, 30, and 31, and as a percentage of sized abalone—either measured or estimated into size bins—for those cycles (see "Methods" section). **Abbreviation**: NR, not recorded]

| Cycle | Year | Site | | | | | | | | | All sites |
| | | 1 | 2 | 3 | 4 | 5 | 6 | 7 | 8 | 9 | |
|---|---|---|---|---|---|---|---|---|---|---|---|
| 31 | 2021 | 0 | 0 | 11 | 2 | 18 | 3 | 17 | 30 | 0 | 81 |
| | | | | (26.4) | (4.8) | (33.3) | (2.0) | (7.8) | (12.6) | | (9.6) |
| Cycle 29 estimated | | 3 | 3 | 0 | 0 | 0 | 0 | 37 | 125 | NR | 168 |
| Cycle 29 percentage including estimated sizes | | (10.1) | (13.5) | (0.0) | (0.0) | (12.5) | (0.0) | (9.1) | (20.5) | NR | (14.4) |
| Cycle 30 estimated | | 0 | 2 | 1 | 0 | 0 | 0 | 74 | 223 | 4 | 304 |
| Cycle 30 percentage including estimated sizes | | (4.0) | (3.7) | (12.8) | (1.9) | (18.8) | (1.8) | (15.0) | (27.5) | (14.3) | (19.0) |
| Cycle 31 estimated | | 7 | 0 | 0 | 1 | 1 | 0 | 59 | 76 | 1 | 145 |
| Cycle 31 percentage including estimated sizes | | (5.0) | (0.0) | (25.6) | (6.3) | (33.9) | (1.9) | (9.8) | (15.0) | (2.2) | (11.2) |
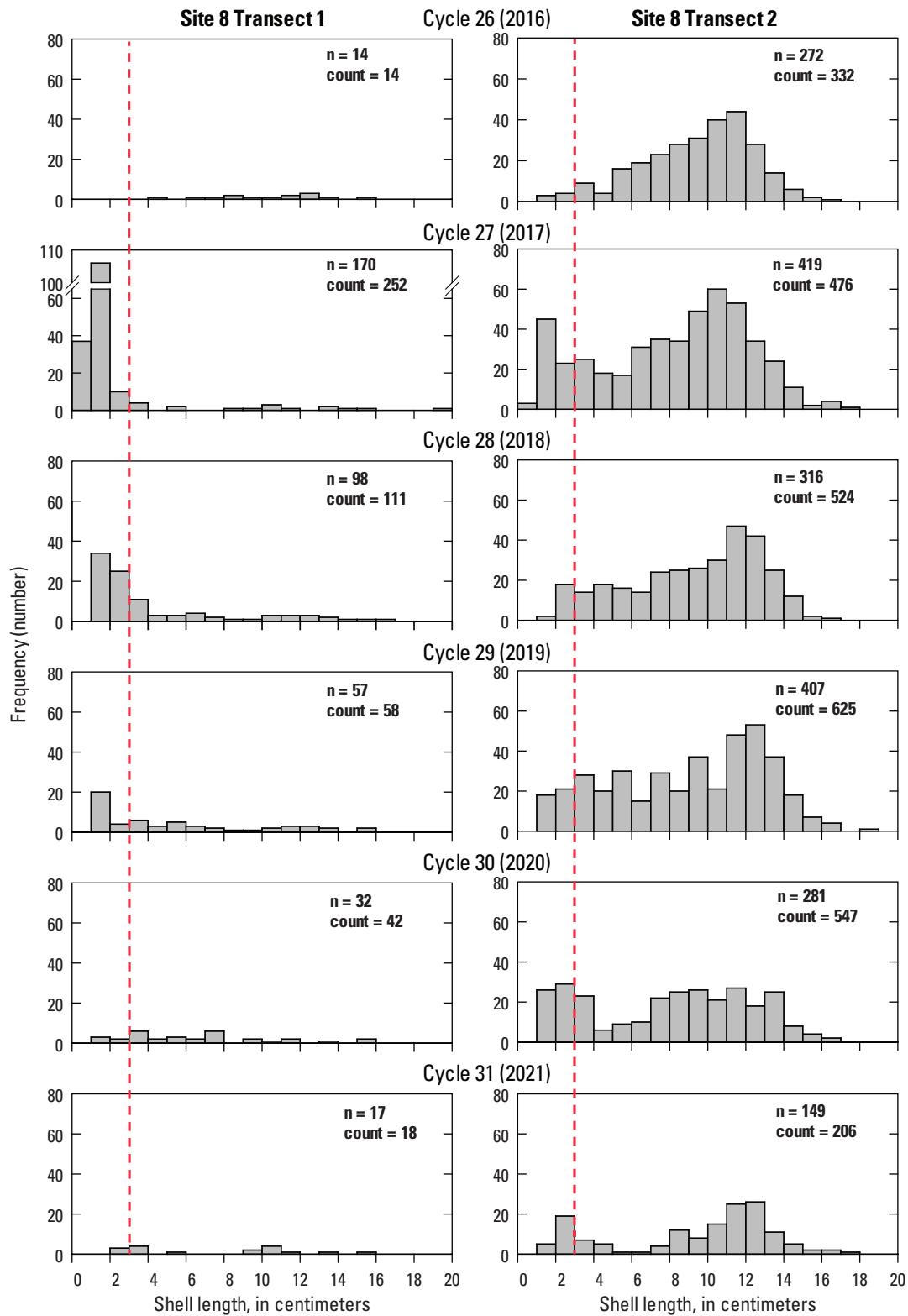
**Figure 13.**    Recruitment pulse as observed in the size distribution measured in 2016–21 at site 8, transects 1 (left) and 2 (right), San Nicolas Island, California. Frequencies are presented here as numbers rather than percentage of sample size. Sizes to the left of the dashed red lines are considered recruits. [n is measured sample size; count is total count on transect]
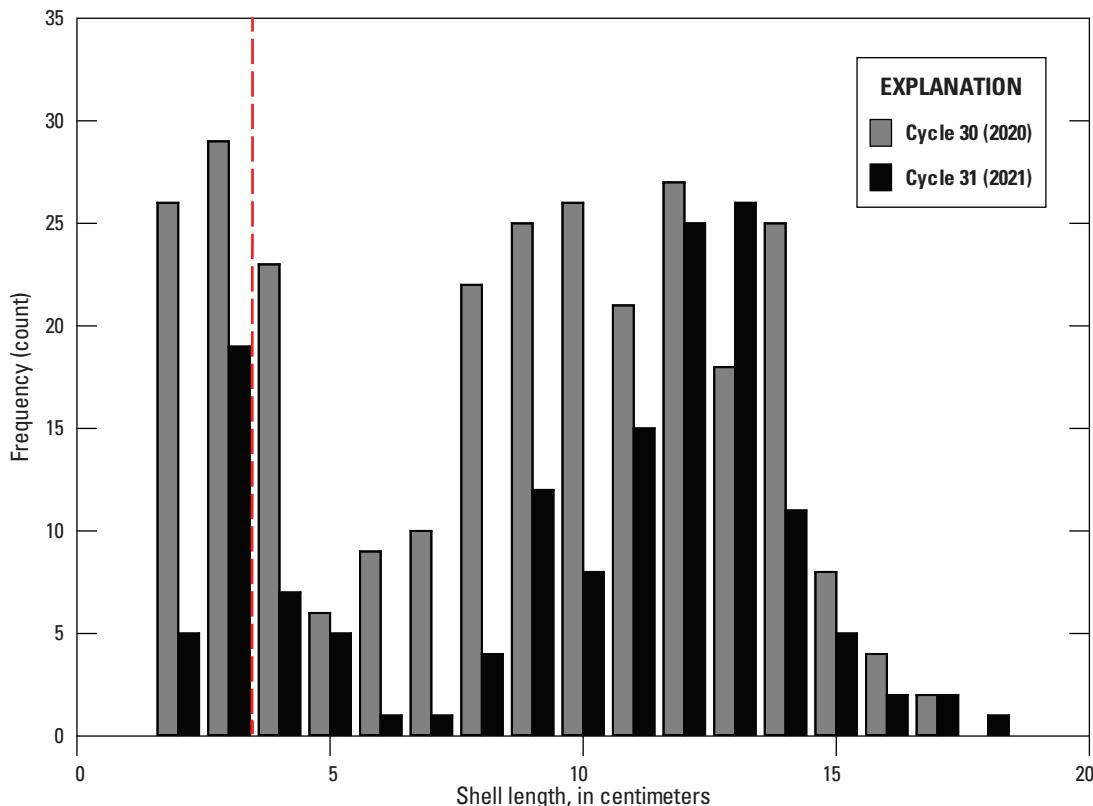
**Figure 14.** Comparison of successive size distributions measured at site 8, transect 2 in 2020 and 2021. Sizes to the left of the dashed red lines are considered recruits.

## Nearest Neighbors

The mean nearest neighbor distance at SNI has been declining for several years as the population size has increased. Figure 15 shows this trend since 2005 when consistent efforts were first made to measure this parameter. The percentage of each sample within 10 cm and within 100 cm of the nearest conspecific are plotted also. The trend for all three metrics is toward closer proximity, and in 2021, 97 percent of the sampled abalone were within 1 meter of another abalone. Proximity should increase the probability of fertilized gametes from a given area (Blaud, 2013).

Figure 16 shows nearest neighbor distance bins plotted by site for 2021. Sites 7 and 8, which dominate in terms of total abalone count, also drive the high numbers in close proximity. These two sites contained 73.0 percent of the counted population, and 90.4 percent of these 1,478 abalone were within 10 cm of another black abalone. In general, the other sites are more evenly spread among the bins, but the other sites still had 67.8 percent of the counted abalone within 10 cm of another.

Table 7 shows the nearest neighbor distance bins assigned to measured abalone that were in the recruit size classes (less than 3.1 cm) for each year from 2005 to 2021. Most recruits, like their adult counterparts, are in the first and second bins, between 0 and 10 cm from other abalone.
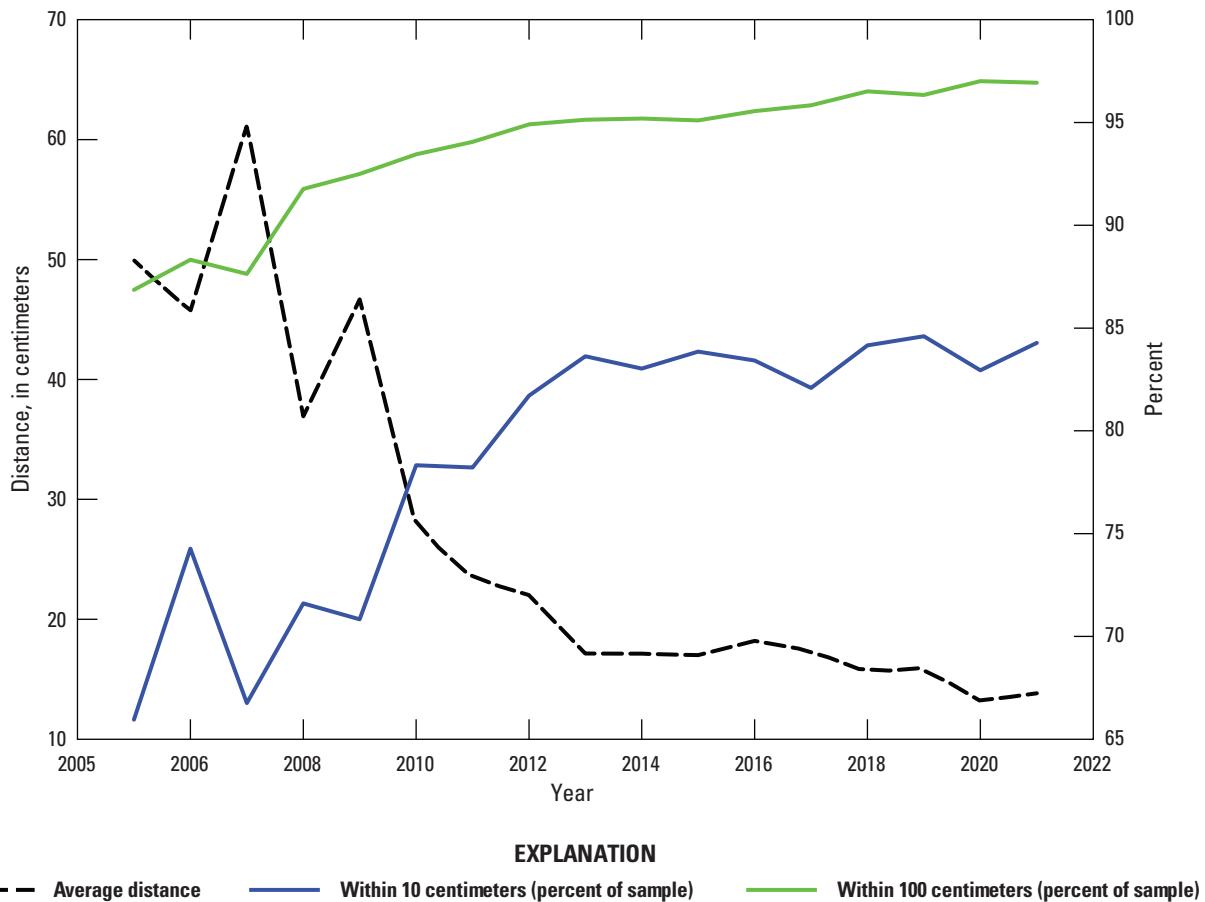
**Figure 15.**    Mean nearest neighbor distance in 2005–21 and percentage of sample within 10 centimeters (cm) and within 100 cm of neighbor, San Nicolas Island, California.
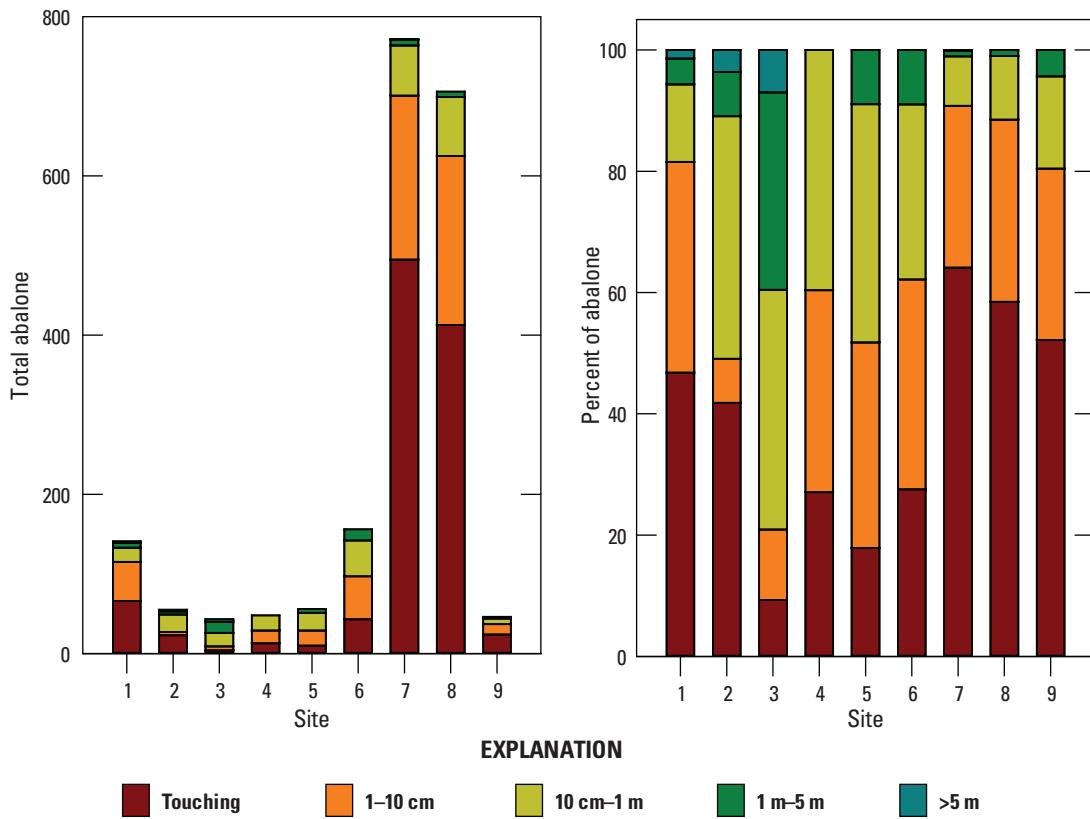
**Figure 16.**     Nearest neighbor distance bins by site for 2021, San Nicolas Island, California. Frequency of bins is shown by number of abalone (left) and by percent of abalone (right).

**Table 7.**    Total black abalone recruits for cycles 15–31 (2005–21) by nearest neighbor distance bin, San Nicolas Island, California.

[Percentage of total (NR excluded) at bottom. Recruits defined as measured individuals with a shell length less than 3.1 centimeters (cm). **Abbreviations**: NR, not recorded; m, meter; >, greater than; —, not applicable]

| Cycle | Year | Nearest neighbor bins | | | | | |
|---|---|---|---|---|---|---|---|
| | | NR | 0 cm | 1–10 cm | 11 cm–1 m | 1–5 m | >5 m |
| 15 | 2005 | 0 | 1 | 1 | 5 | 0 | 0 |
| 16 | 2006 | 6 | 3 | 12 | 2 | 1 | 0 |
| 17 | 2007 | 0 | 2 | 0 | 1 | 0 | 0 |
| 18 | 2008 | 0 | 8 | 11 | 9 | 1 | 0 |
| 19 | 2009 | 0 | 6 | 9 | 6 | 1 | 0 |
| 20 | 2010 | 0 | 39 | 48 | 19 | 4 | 0 |
| 21 | 2011 | 2 | 72 | 31 | 12 | 7 | 0 |
| 22 | 2012 | 1 | 8 | 7 | 5 | 1 | 1 |
| 23 | 2013 | 0 | 22 | 18 | 12 | 4 | 0 |
| 24 | 2014 | 0 | 30 | 22 | 12 | 3 | 1 |
| 25 | 2015 | 0 | 40 | 27 | 9 | 8 | 0 |
| 26 | 2016 | 2 | 47 | 32 | 8 | 3 | 1 |
| 27 | 2017 | 2 | 125 | 129 | 59 | 14 | 3 |
| 28 | 2018 | 0 | 64 | 31 | 9 | 4 | 0 |
| 29 | 2019 | 0 | 58 | 22 | 9 | 2 | 1 |
| 30 | 2020 | 0 | 68 | 35 | 24 | 4 | 0 |
| 31 | 2021 | 0 | 30 | 26 | 14 | 10 | 1 |
| Total for all cycles | | | | | | | |
| — | — | — | 623 | 461 | 215 | 67 | 8 |
| Percentage for all cycles | | | | | | | |
| — | — | — | 45.3 | 33.6 | 15.6 | 4.9 | 0.6 |

## Sedimentation

Sand cover in the quadrats did not reveal an obvious trend temporally or by transect. Figure 17 shows mean sand cover for selected transects (those with generally higher cover) and total mean sand cover, over time, from 2001 to 2021. No multi-year trend is apparent but inter-year and inter-transect variation are obvious. There seems to be only weak synchrony between the transects although, in 2016, several appeared to peak in sand cover. Ironically, for the one site where it is thought that sand burial caused mass mortality of black abalone (decline recorded winter 2016, site 3, transects 1 and 2), there was zero sand cover in the data. The sand cover there was apparently brief and catastrophic. The sites more typically influenced by sand are 1, 7, and 8. In 2021, sand cover increased at site 1 but decreased at sites 7 and 8.

A sand intrusion event was noted in 2020 at site 7, transect 4 that resulted in some redistribution of abalone but no measured decline. This transect had vertical rock faces that acted as refugia for abalone able to climb above the sand surface. In 2021, the sand was completely gone from this transect. How sand cover affects abalone is likely to be a result of several factors, including depth of burial, duration of the event, and the availability of protruding rock refugia.
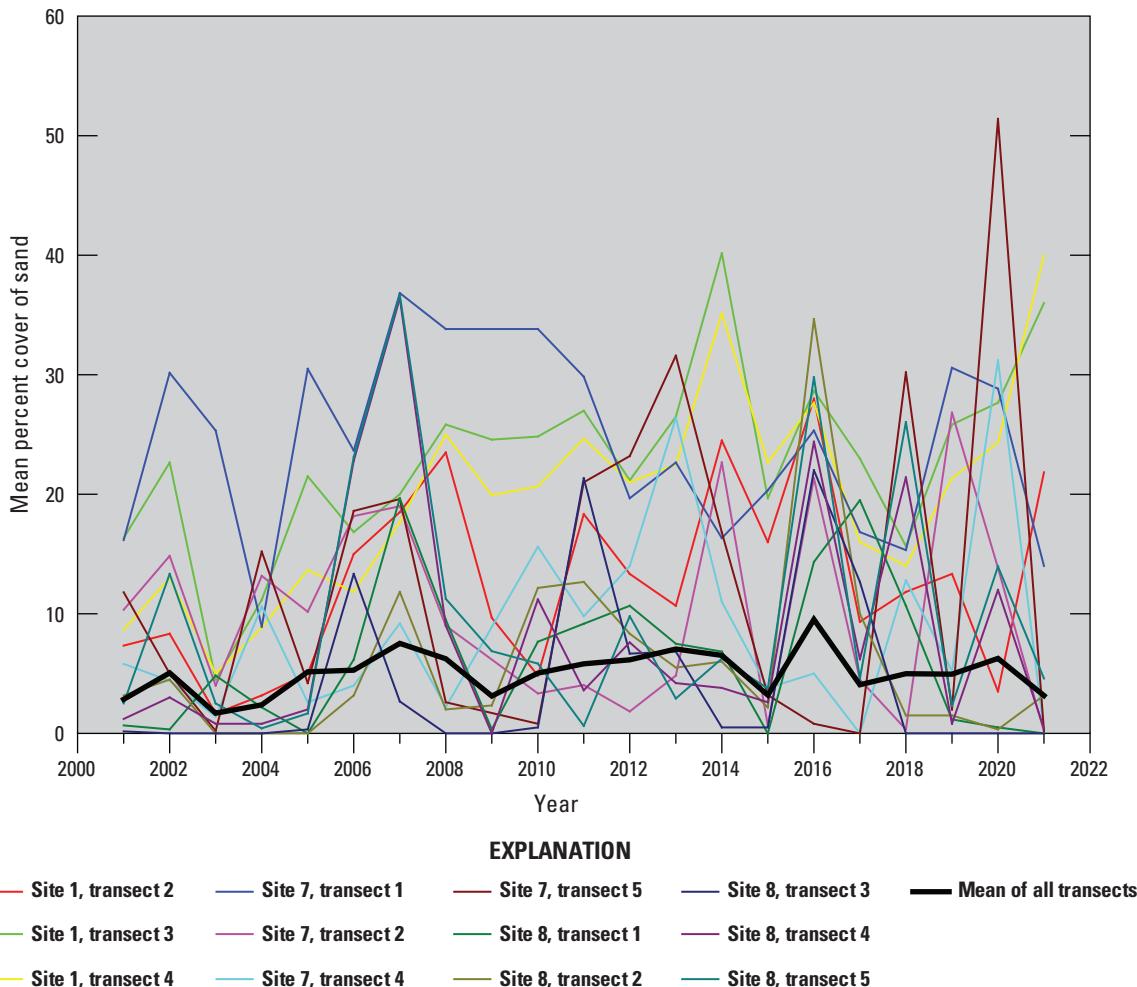


**Figure 17.**   Average sand cover on selected transects for 2001–21, San Nicolas Island, California. Heavy black line shows total mean cover over time.

# Conclusion

The decline in the total San Nicolas Island black abalone count for all sites combined in 2021 seems at first glance to be a correction after the 15.8 percent increase observed in 2020 (table 3). The count is almost identical to the total in 2019 and very similar to those from 2017 and 2018. However, when viewed at the site or transect level it is apparent that the cause of the decline may be isolated to site 8, transect 2. This transect also experienced a decline of 78 abalone the previous year (table 2).

The cause, or causes, of the decline in abundance on this transect is unclear. The change in size distribution indicates that the largest declines occurred in the size classes less than 11 centimeters (fig. 14). An examination of microhabitat usage indicates all the loss was from the preferred crevice habitat with the number of abalone using open habitat increasing slightly from 24 to 37. The 2021 field season was unusual in that most of the transects were sampled in full dark, with the remainder sampled under growing light conditions of dawn. Although the dark made navigating the intertidal more difficult, the consensus among the observers was that the focus of light from headlamps and lack of ambient light made it easier to thoroughly search quadrats, particularly crevice habitat. Because sampling in the dark did not appear to reduce sight ability of abalone and because most of the lower counts were at one or two transects, it seems unlikely that these sampling conditions were a cause of the lower count numbers.

Although empty shells were found near the transect, they were not unusually abundant. There is no indication that sand burial, which has been seen or suspected of causing black abalone mortality, was a factor here. In fact, owing to the structure and location of transect 2, sand burial seems very unlikely. The possibility of a localized outbreak of withering syndrome (WS) cannot be dismissed but there is no direct evidence of one. Alternatively, given the size selective nature of the decline, predation by octopus or other abalone predators is a possibility.

The island-wide recruitment rate of 9.6 percent was typical for the last few years (fig. 11). The 10-year average from 2011 to 2020 was 11.2 percent (4.0–26.5). The highest recruitment rate was observed in 2017 when six of the sites had rates above 10 percent and recruits were recorded at all sites except site 2; however, the ultimate lack of population growth at two transects at site 8, discussed earlier, indicates that even large recruitment events may not always result in population growth. If the suitable numbers of recruits don't survive to reproductive size, they don't contribute to the population.

Data from recent years indicate that a higher percentage of abalone inhabit crevice habitat than before WS. The greater utilization of exposed microhabitats that was observed before WS was likely a result of crowding of the more preferred crevice habitats when the population size was at unnaturally high levels because of the absence of sea otters and most human predation. Compared with those in open habitat, abalone in crevice habitat likely experience temperatures that are less extreme at low tide (G.R. VanBlaricom, U.S. Geological Survey, unpub. data, 2007). Crevice habitat may also confer an advantage in drift capture by funneling water containing drift material past resident abalone. Finally, crevices can help protect abalone from dislodgement by wave-born projectiles, such as boulders or logs, and can provide a refuge from some predators, like sea otters. It is unclear if predation by sea otters is helping to shape the apparent microhabitat choice, but sites 6 and 4, the sites showing the lowest proportion of crevice utilization in the last two decades, are relatively flat sites, indicating that availability is an important factor in the microhabitat distribution.

Most black abalone recruits were detected within 10 centimeters of other abalone. Whether this pattern is a result of settlement cues or some other phenomenon, such as migration or differential survival, is unclear, but this apparent intra-species fidelity, though ultimately favorable for spawning success, could tend to limit resettlement of unoccupied areas. However, of the 20 transects that had no abalone on them in 2001, only 4 transects had no abalone in 2021 and all 31 transects that had no abalone at some point during the last 20 years later had some abalone on them. This data indicates that recolonization is possible and was ongoing. Immigration onto transects was probably at least as important as recruitment for these recoveries, which is evidenced by the increased numbers of larger abalone at site 1.

The significance of the decline recorded at the most populous site is difficult to minimize. Although there have been greater percentage reductions at other sites in the last several years, the loss of 397 abalone at a site has not been observed since the 1990s when populations were declining because of WS. Despite this decline, the monitored population at San Nicolas Island was still 10 times the size it was 20 years earlier; all but one of the sites had higher counts than in 2016, which is the last time there was a decline in the total count. Out of the nine sites, three had overall densities above one per square meter, and regular recruitment continued to occur at most of the sites.

# References Cited

Blaud, B.M., 2013, Spatial and temporal patterns of fertilization in black abalone (*Haliotis cracherodii* Leach, 1814)—Analysis of surrogate gamete spawning experiments with application towards populations on San Nicolas Island: California, University of Washington.

Boolootian, R.A., Farmanfarmaian, A., and Giese, A.C., 1962, On the reproductive cycle and breeding habits of two western species of *haliotis*: The Biological Bulletin, v. 122, no. 2, p. 183–193, accessed August 23, 2022, at https://doi.org/10.2307/1539587.

California Department of Fish and Game, 2004, Annual status of the fisheries report through 2003—Report to the Fish and Game Commission as directed by the Marine Life Management Act of 1998: California Department of Fish and Game Marine Region, 182 p.

Chambers, M.D., VanBlaricom, G.R., Hauser, L., Utter, F., and Friedman, C.S., 2006, Genetic structure of black abalone (*Haliotis cracherodii*) populations in the California islands and central California coast—Impacts of larval dispersal and decimation from withering syndrome: Journal of Experimental Marine Biology and Ecology, v. 331, no. 2, p. 173–185, accessed August 23, 2022, at https://doi.org/10.1016/j.jembe.2005.10.016.

Friedman, C.S., Biggs, W., Shields, J.D., and Hedrick, R.P., 2002, Transmission of withering syndrome in black abalone, *Haliotis cracherodii* Leach: Journal of Shellfish Research, v. 21, no. 2, p. 817–824.

Friedman, C.S., Wight, N., Crosson, L.M., VanBlaricom, G.R., and Lafferty, K.D., 2014, Reduced disease in black abalone following mass mortality—Phage therapy and natural selection: Frontiers in Microbiology, v. 5, no. 78, 10 p., accessed August 23, 2022, at https://doi.org/10.3389/fmicb.2014.00078.

Hastie, T.J., and Pregibon, D., 1992, Generalized linear models, *in* Chambers, J.M., and Hastie, T.J., eds., Statistical models in S: Pacific Grove, Calif., Wadsworth & Brooks/Cole.

Kenner, M.C., 2020, Black abalone surveys at Naval Base Ventura County, San Nicolas Island, California—2019, annual report: U.S. Geological Survey Open-File Report 2020–1047, 41 p., accessed August 23, 2022, at https://doi.org/10.3133/ofr20201047.

Lafferty, K.D., and Kuris, A.M., 1993, Mass mortality of abalone *Haliotis cracherodii* on the California Channel Islands—Tests of epidemiological hypotheses: Marine Ecology Progress Series, v. 96, p. 239–248, accessed August 23, 2022, at https://doi.org/10.3354/meps096239.

Leighton, D., and Boolootian, R.A., 1963, Diet and growth in the black abalone, *Haliotis cracerodii*: Ecology, v. 44, no. 2, p. 227–238, accessed August 23, 2022, at https://doi.org/10.2307/1932170.

Miner, C.M., Altstatt, J.M., Raimondi, P.T., and Minchinton, T.E., 2006, Recruitment failure and shifts in community structure following mass mortality limit recovery prospects of black abalone: Marine Ecology Progress Series, v. 327, p. 107–117, accessed August 23, 2022, at https://doi.org/10.3354/meps327107.

Morris, R.H., Abbott, D.P., and Haderlie, E.C., 1980, Intertidal invertebrates of California: Stanford, Calif., Stanford University Press.

National Marine Fisheries Service, 2020, Final Endangered Species Act recovery plan for black abalone (*Haliotis cracherodii*): Long Beach, Calif., National Marine Fisheries Service, West Coast Region, Protected Resources Division, 93 p., accessed August 23, 2022, at https://www.fisheries.noaa.gov/species/black-abalone#conservation-management.

National Oceanic and Atmospheric Administration, 2009, Endangered and threatened wildlife and plants—Endangered status for black abalone: Federal Register, v. 74, no. 9, p. 1937–1946, accessed August 23, 2022, at https://www.govinfo.gov/content/pkg/FR-2009-01-14/pdf/E9-635.pdf.

National Oceanic and Atmospheric Administration, 2011, Endangered and threatened wildlife and plants—Final rulemaking to designate critical habitat for black abalone: Federal Register, v. 76, no. 208, p. 66806–66844, accessed August 22, 2022, at https://www.govinfo.gov/content/pkg/FR-2011-10-27/pdf/2011-27376.pdf.

Neuman, M., Tissot, B., and Vanblaricom, G., 2010, Overall status and threats assessment of black abalone (*Haliotis cracherodii* Leach, 1814) populations in California: Journal of Shellfish Research, v. 29, no. 3, p. 577–586, accessed August 22, 2022, at https://doi.org/10.2983/035.029.0305.

R Core Team, 2017, R—A language and environment for statistical computing: Vienna, Austria, R Foundation for Statistical Computing, accessed August 22, 2022, at https://www.R-project.org.

Raimondi, P.T., Wilson, C.M., Ambrose, R.F., Engle, J.M., and Minchinton, T.E., 2002, Continued declines of black abalone along the coast of California—Are mass mortalities related to El Niño events?: Marine Ecology Progress Series, v. 242, p. 143–152, accessed August 22, 2022, at https://doi.org/10.3354/meps242143.

Rathbun, G.B., Hatfield, B.B., and Murphey, T.G., 2000, Status of translocated sea otters at San Nicolas Island, California: The Southwestern Naturalist, v. 45, no. 3, p. 322–328, accessed August 22, 2022, at https://doi.org/10.2307/3672835.

Rick, T.C., Vellanoweth, R.L., Erlandson, J.M., and Kennett, D.J., 2002, On the antiquity of the single-piece shell fishhook—AMS radiocarbon evidence from the Southern California Coast: Journal of Archaeological Science, v. 29, no. 9, p. 933–942, accessed August 22, 2022, at https://doi.org/10.1006/jasc.2001.0788.

U.S. Navy, 2015, Integrated natural resources management plan for Naval Base Ventura County, San Nicolas Island, California—December 2010 [updated December 2015]: San Diego, Calif., Naval Base Ventura County, San Nicolas Island, Environmental Division and Naval Facilities Engineering Command, Southwest, 1760 p.

VanBlaricom, G.R., 1993, Dynamics and distribution of black abalone populations at San Nicolas Island—Third California Islands Symposium—Recent advances in research on the California Islands: Santa Barbara, Calif., Santa Barbara Museum of Natural History, p. 323–334.

VanBlaricom, G.R., and Kenner, M.C., 2020, Dietary patterns in black abalone *Haliotis cracherodii* Leach, 1814 as indicated by observation of drift algal and seagrass capture at San Nicolas Island, California, USA, 1982 to 2019: Journal of Shellfish Research, v. 39, no. 1, p. 113–124, accessed August 22, 2022, at https://doi.org/10.2983/035.039.0111.

VanBlaricom, G.R., Ruediger, J.L., Friedman, C.S., Woodard, D.D., and Hedrick, R.P., 1993, Discovery of withering syndrome among black abalone *Haliotis cracherodii* Leach, 1814, populations at San Nicolas Island, California: Journal of Shellfish Research, v. 12, p. 185–188.

VanBlaricom, G.R., Neuman, M., Butler, J., DeVogelaere, A., Gustafson, R.R., Mobley, C., Richards, D., Rumsey, S., and Taylor, B.L., 2009, Status review report for black abalone: Long Beach, Calif., National Marine Fisheries Service Southwest Region, 135 p.

Watson, J., 2000, The effects of sea otters (*Enhydra lutris*) on abalone (*Haliotis* spp.) populations, *in* Campbell, A., ed., Workshop on rebuilding abalone stocks in British Columbia: Canadian Special Publication of Fisheries and Aquatic Sciences, v. 130, p. 123–132.

Webber, H.H., and Giese, A.C., 1969, Reproductive cycle and gametogenesis in the black abalone *Haliotis cracheroidii* (Gastropoda—Prosobranchiata): Marine Biology, v. 4, no. 2, p. 152–159, accessed August 22, 2022, at https://doi.org/10.1007/BF00347041.

Wood, S.N., 2017, Generalized additive models—An introduction with R (2d ed.): New York, Chapman and Hall/CRC, 496 p., accessed August 22, 2022, at https://doi.org/10.1201/9781315370279.

USGS